

ISTANBUL TECHNICAL UNIVERSITY ★ GRADUATE SCHOOL OF SCIENCE
ENGINEERING AND TECHNOLOGY

CELL SEPARATION IN MICROFLUIDIC CHANNELS

M.Sc. THESIS

Merve ZUVİN

Department of Nanoscience & Nanoengineering

Nanoscience & Nanoengineering Programme

JUNE 2013

ISTANBUL TECHNICAL UNIVERSITY ★ GRADUATE SCHOOL OF SCIENCE
ENGINEERING AND TECHNOLOGY

CELL SEPARATION IN MICROFLUIDIC CHANNELS

M.Sc. THESIS

Merve ZUVİN
(513101011)

Department of Nanoscience & Nanoengineering

Nanoscience & Nanoengineering Programme

Thesis Advisor: Prof. Dr. Levent TRABZON

JUNE 2013

İSTANBUL TEKNİK ÜNİVERSİTESİ ★ FEN BİLİMLERİ ENSTİTÜSÜ

MİKRO KANALLARDA HÜCRE AYRIŞTIRMA

YÜKSEK LİSANS TEZİ

**Merve ZUVİN
(513101011)**

Nanobilim & Nanomühendislik Anabilim Dalı

Nanobilim & Nanomühendislik Programı

Tez Danışmanı: Prof. Dr. Levent TRABZON

HAZİRAN 2013

Merve ZUVİN, a **M.Sc.** student of ITU **Graduate School of Science Engineering and Technology** student ID 513101011 successfully defended the **thesis** entitled “**CELL SEPARATION IN MICROFLUIDIC CHANNELS**”, which she prepared after fulfilling the requirements specified in the associated legislations, before the jury whose signatures are below.

Thesis Advisor : **Prof. Dr. Levent TRABZON**

İstanbul Technical University

Jury Members : **Assoc. Prof. Dr. Hüseyin KIZIL**

İstanbul Technical University

Assoc. Prof. Dr. Erdem ALACA

Koç University

Date of Submission : 3 May 2013
Date of Defense : 7 June 2013

To my family,

FOREWORD

I would like to thank my advisor Prof. Dr. Levent TRABZON and Assoc. Prof. Dr. Hüseyin KIZIL for giving me the opportunity to be a part of their team and being supportive for me to study the subject I wanted.

I would like to thank Prof. Dr. Oğuz ÖZTÜRK and Mete Bora Tüzüner, M.Sc. for providing cell lines.

I would like to thank Assoc. Prof. Dr. Ayça SAYI YAZGAN and Nesteren MANSUR for cell culture and flow cytometry analysis.

I also would like to thank Mümin BALABAN, Mustafa YILMAZ, M.Sc., Arzu ÖZBEY, M.Sc., Alperen ACEMOĞLU, Muhammed BEKİN and all the ITUMEMS Lab members for their help and support and Semra Zuhale FİCEN BİROL, M.Sc. for sharing her knowledge and her support.

I would like to thank my parents Hilal ZUVİN and Mehmet ZUVİN, my brother Safa Mert ZUVİN, my aunt Meral KARDEŞKAYA for their support, patience and love.

May 2013

Merve ZUVİN
(Physicist)

TABLE OF CONTENTS

	<u>Page</u>
FOREWORD	ix
TABLE OF CONTENTS	xi
ABBREVIATIONS	xiii
LIST OF TABLES	xv
LIST OF FIGURES	xvii
SUMMARY	xix
ÖZET	xxiii
1. INTRODUCTION	1
1.1 Literature Review	2
2. THEORY	11
2.1 Inertial Microfluidics.....	11
2.2 Dean Secondary Flow	12
3. MATERIALS AND METHOD	15
3.1 Fabrication of the Microfluidic Device	15
3.1.1 SU-8 photoresist.....	15
3.1.2 Acetate mask fabrication.....	15
3.1.3 Fabrication of master mold	16
3.2 Channel Fabrication	18
3.2.1 PDMS casting	18
3.2.2 O ₂ plasma treatment	19
3.3 Experimental	20
3.3.1 Depth analysis	20
3.3.2 Optical microscope analysis.....	20
3.3.3 Design	21
3.3.4 Flow cytometer	23
3.3.5 Cell mixture.....	24
4. RESULTS AND DISCUSSION	27
4.1 Determining Required Flow Rates	27
4.2 CFSE Labeled MCF7 and Unlabeled MDA-MB-231 Mixture Experiments ..	30
4.2.1 400 µm wide channel	30
4.2.2 500 µm wide channel	32
4.2.3 600 µm wide channel	33
4.2.4 700 µm wide channel	36
5. CONCLUSIONS AND RECOMMENDATIONS	39
REFERENCES	41
CURRICULUM VITAE	45

ABBREVIATIONS

MEMS : Micro Electro Mechanical Systems
PDMS : Polydimethyl Siloxane
 μ TAS : Micro Total Analysis System
POC : Point-of -Care
DEP : Dielectrophoresis
SEM : Scanning Electron Microscopy
 a_p : Particle Diameter
 C_L : Lift Coefficient
 D_e : Dean Number
 D_h : Channel Hydraulic Diameter
 F_D : Dean Drag Force
 F_L : Net Lift Force
H : Channel Height
W: Channel Width
 μ : Dynamic Viscosity
Re: Reynolds Number
 U_f : Fluid Velocity
FR : Flow Rate
CFSE : Carboxyfluorescein Succinimidyl Ester
PBS : Phosphate Buffered Saline

LIST OF TABLES

	<u>Page</u>
Table 3.1 : Soft Bake Times.....	17
Table 3.2 : Thickness and Exposure Energy.....	17
Table 3.3 : Post Exposure Bake Times.	18
Table 3.4 : Development Times.	18
Table 3.5 : Channel Height – Channel Width Table.....	22
Table 3.6 : Focus Parameters According to Theoretical Calculations	22
Table 4.1 : Flow rates – Dean numbers.....	28

LIST OF FIGURES

	<u>Page</u>
Figure 1.1: Interactions between techniques and materials	2
Figure 1.2 : SEM image of pillars	3
Figure 1.3 : SEM images A) Commercial pored membrane B) Parylene filter C-D) Captured cells	4
Figure 1.4 : Separation principle of device	5
Figure 1.5 : (a) : Particle experiment (b) Cell experiment	5
Figure 1.6 : SEM images of microfluidic device a) 50 nm pillars b) 50 nm perpendicular lines c) 50 nm parallel lines d) image of microfluidic channel e) image of nanopatterned region	6
Figure 1.7 : A) Principle of device B) PDMS microchip C) Magnetically assembled array D) Jurkat cells E) Raji cells	8
Figure 1.8 : Image of captured lung cancer cells from blood	9
Figure 2.1 : F_{Wall} and F_{Shear} effects	11
Figure 2.2 : Dean flow in curved channels.	13
Figure 2.3 : Forces acting on a particle in curved channels.	13
Figure 3.1 : Acetate Mask.	15
Figure 3.2 : Thickness vs Spin Speed (21°C)	16
Figure 3.3 : Schematic illustration of PDMS channel production	19
Figure 3.4 : Profilometer analysis result.	20
Figure 3.5 : Optical microscope image of a defected channel.	21
Figure 3.6 : Channel design and outlet positions.	21
Figure 3.7 : Channel outlet positions in microscope image.	22
Figure 3.8 : Flow Cytometry Mechanism	23
Figure 3.9 : Flow Cytometer Data.	24
Figure 3.10 : Fluorescent dye efficiencies.	25
Figure 3.11 : Cell mixture flow cytometer analysis.	25
Figure 4.1 : Focus images of 400 – 700 μm wide channels due to flow rates.	27
Figure 4.2 (continued) : Focus images of 400 – 700 μm wide channels due to flow rates.	28
Figure 4.3 : Flow cytometer results of three outlets.	29
Figure 4.4 : Focus possibilities due to flow rates at 400 μm wide channel.	30
Figure 4.5 : 400 μm wide channel flow cytometer results.	31
Figure 4.6 : Focus possibilities due to flow rates at 500 μm wide channel.	32
Figure 4.7 : 500 wide channel flow cytometer results	33
Figure 4.8 : Focus possibilities due to flow rates at 600 μm wide channel	34
Figure 4.9 : 600 wide channel flow cytometer results.	35
Figure 4.10 : Focus possibilities due to flow rates at 700 μm wide channel.	36
Figure 4.11 : 700 μm wide channel flow cytometer results.	37

CELL SEPARATION IN MICROFLUIDIC CHANNELS

SUMMARY

Microfabrication has recently found many advanced application areas in. Microfluidics has been becoming widely used in molecular and cellular biology. Microfluidic chips provide fast and exact diagnosis due to their realibility and controllable capabilities. Miniaturizing provides us many advantages in diagnostic device such as use of small amount of samples, fast reaction time, and different types of tests in one chip and cheapness. Microfluidics can be applied to various segments of biological detection from DNA separation to infectious disease detection.

Several methods were developed to perform these kinds of tests in microfluidics. Filtration and enrichment procedures are very important for many chemical and biological applications. Microfluidics achieve these goals with two different methods which are active methods using external forces in seperation of microparticles and passive ones utilizing fludic inertial forces. These external forces can be electric field, magnetic field or optical stimulus. It is demonstrated that active systems yield higher efficiencies however their need to external power supply limits their portability and raising the cost of their use. In this thesis it is aimed to design and produce an alternative device for conventional diagnostic methods.

Passive methods without any external forces are the ones which is seperating microparticles by means of flow regime. Important parameter is the geometry of design to manipulate particle or cells via fluence of channel geometry on carrier fluid thereby particle or cell as well. A particle in a solution experience drag and lift forces, primarily. Drag force effects the particle in flow direction and make the particle migrate through the channel. Lift forces acting on a particle are perpendicular to flow direction and play role in sorting. Lift forces effect the particle in two ways. One of these effects is shear induced lift force which drags the particles through the wall from the center. Other effect is wall induced lift force which pushes the particle away from the wall to the center. This is the focus principle in straight channels. It is observed that with addition of curved shapes to channel geometry, particles experience a secondary force as well. This force is caused by the velocity mismatch between center and near center regions in flow direction. When it is looked at the cross-section, two opposite directioned vortices are observed at the top and bottom of the channel and they lead particles to move circular through the cross-section path. This force is called Dean force. Particles start to be located at equilibrium positions where Dean force and the balance of two primary lift forces are equal and afterwards focusing which is needed for sorting begins. Important parameters are channel dimensions, particle diameter and flow rate. Because of Dean force, curved channels yield faster reaction times and it makes it possible to work with shorter channels.

Fabrication of microchannels is generally performed by using soft lithography techniques. Designed patterned is formed onto Si-wafer by using UV light sensitive polymer material (photoresist) via optical lithography and the main material, PDMS,

is poured onto patterned Si-wafer and peeled off after solidification. When channel is stucked to the glass after plasma treatment, microchip is fabricated. PDMS is cheap, non-toxic and biocompatible material and it is widely used in microchannel applications.

In this work, Dean force coupled curved microchannels were designed for concentration of MCF7 human breast cancer cells from a suspension that contains MDA-MB-231 (~ 15 μm in diameter) and MCF7 (~ 20 μm in diameter) human breast cancer cell lines. Channels which have height x width 81 μm x 400 μm , 84 μm x 500 μm , 91 μm x 600 μm and 86 μm x 700 μm dimensions were fabricated. Channels had one inlet and three outlets. After culturing both MCF7 and MDA-MB-231 cells, target cell –MCF7- has stained with two different fluorescent dye and effectiveness of these dyes were investigated with flow cytometry. Then, a million labeled MCF7 and a million unlabeled MDA-MB-231 cells were mixed in 100 ml PBS solution. 20 ml cell suspension was used for each experiment. It was observed that high flow rates are required for focusing of MCF7 cells. Experiments showed that MCF7 enrichment at the second outlets of each channel and it was confirmed with flow cytometry analysis. Then another group of MCF7 cells were stained with another fluorescent dye for second experimental group and more flow rate values were investigated.

400 μm wide channel experiment was performed at 1000 – 1500 – 1700 – 2500 $\mu\text{l}/\text{min}$, respectively and focus positions for each flow rate were investigated with optical microscope images and intensity analysis. Results were confirmed with flow cytometry and according to these data, there was no focus at 1000 $\mu\text{l}/\text{min}$. At 1500 $\mu\text{l}/\text{min}$ MCF7 cells tended to equilibrate in one direction and at 1700 and 2500 $\mu\text{l}/\text{min}$ focusing of MCF7 cells were observed.

500 μm wide channel experiment was performed at 1500 – 2000 – 2500 $\mu\text{l}/\text{min}$, respectively and focus positions for each flow rate were investigated with optical microscope images and intensity analysis. Results were confirmed with flow cytometry and according to these data, there is no focus at 1500 $\mu\text{l}/\text{min}$. At 2000 $\mu\text{l}/\text{min}$ MCF7 cells tend to equilibrate in one direction and at 2500 $\mu\text{l}/\text{min}$ focusing of MCF7 cells were observed.

600 μm wide channel experiment was performed at 2000 – 2500 – 3000 - 3500 $\mu\text{l}/\text{min}$, respectively and focus positions for each flow rate were investigated with optical microscope images and intensity analysis. Results were confirmed with flow cytometry and according to these data there is no focus at 2000 $\mu\text{l}/\text{min}$. At 2500 $\mu\text{l}/\text{min}$ MCF7 cells tend to equilibrate in one direction and at 3000 and 3500 $\mu\text{l}/\text{min}$ focusing of MCF7 cells were observed.

700 μm wide channel experiment was performed at 2500 – 3000 - 3500 $\mu\text{l}/\text{min}$, respectively and focus positions for each flow rate were investigated with optical microscope images and intensity analysis. However no focus positions were observed for these flow rates. Flow cytometry analysis showed that there are MCF7 cells at each three outlets and enrichment could not be achieved. Higher than 3500 $\mu\text{l}/\text{min}$ flow rates were required to focus MCF7 cells but it was not performed due to technical problems with syringe pump.

Enrichment at appropriate flow rates were achieved by means of channels which were produced within this thesis. Thus, one type of cell population was enriched and distinguished from a cell mixture that contains two different types of cells. These curved channels can be regarded as a prototype of a microfluidic diagnostic device

with their fast reaction time, relatively accurate results, cost effective and miniaturized features.

MİKROKANALLARDA HÜCRE AYRIŞTIRMA

ÖZET

Mikroüretim biyolojide kendine geniş çapta birçok uygulama alanı bulmuştur. Mikroakışkanlar moleküler ve hüresel biyolojide geniş alanda kullanılır hale gelmiştir. Mikroçipler hızlı ve doğru teşhis sağlayabilen ucuz tanı cihazlarıdır. Bir tanı cihazını küçük boyutlara indirmek az miktarda örnek gerektirmesi, hızlı cevap alabilme ve bir çipte farklı testler yapabilme olanağı vermesi dolayısıyla birçok fayda sağlar. Bu cihazlar testleri daha iyi koşullarda yapmaya olanak verir ve maliyeti düşürürken bakımın kalitesini artırır.

Mikroakışkanlar DNA, RNA'dan bulaşıcı hastalık teşhisine kadar birçok alanda uygulanabilir. Bu çalışma ise özel olarak kanser teşhisine yöneliktir ve bunun yanında diğer alanlarla da ilgili, uygulama bazlı literatür araştırmasına yer verilmiştir.

Diğer hastalıklarla karşılaştırıldığında kanser birçok yönden farklılık gösterir. Kanser yapısının karakterizasyonunun, hatta büyüme mekanizmasının birinden diğerine farklılık göstermesi büyük bir klinik problemdir. Kanser, dünyada hala en çok korkulan hastalıktır. Hastalığın gidişatını öngörebilmek ve hastanın hayatta kalmasını sağlayabilmek için kanserin erken teşhisi çok önemlidir. Bu yüzden erken teşhis için hassas ve özel yöntemler geliştirmek çok önemlidir. İnvazif olmayan, ucuz, çok fonksiyonlu karakterizasyon cihazları geliştirmek hastalığı daha iyi bir şekilde izlemek, daha verimli tanısall görüntüleme olanakları sağlayacaktır.

Tüm bu amaçları gerçekleştirmek için mikroakışkan alanında çeşitli yöntemler geliştirilmiştir. Filtreleme işlemleri birçok kimyasal ve biyolojik uygulama için çok önemlidir. Bundan dolayı MEMS teknikleri ile de parçacık veya hücre ayırıştırma, filtreleme ve zenginleştirme çalışmaları geliştirilmektedir. Mikroakışkan alanının da bu iki yolla yapılır. Bunlar dış etken kullanılan aktif yöntemler ve dış etken kullanılmayan pasif yöntemlerdir. Aktif yöntemlerde parçacığın uygulanan dış kuvvete verdiği cevapla ayırma sağlanır. Bu dış kuvvet elektrik alan, manyetik alan ya da optik bir uyarıcı olabilir. Bu yöntemlerin daha yüksek verimle çalıştığı gösterilmiştir ancak dış bir güç kaynağına duyulan ihtiyaç onların taşınabilir olma özelliğini kısıtlarken bu teçhizatların pahalı olması nedeniyle maliyeti de artırmaktadır.

Pasif yöntemlerde ise dış etkiye gerek duyulmaksızın ayırma sağlanır. Buradaki en önemli parametre tasarlanan mikrokanalın geometrisi ve kanalın taşıyıcı sıvı üzerindeki etkisinin parçacık ya da hücre manipülasyonu sağlanacak şekilde etki ettirilmesidir. Bir mikrokanalda sıvı içerisindeki bir parçacığa öncelikle sürüklenme ve kaldırma kuvvetleri etki eder. Sürüklenme kuvveti akış yönünde etki eder ve parçacıkların kanal boyunca ilerlemesini sağlar. Kaldırma kuvvetleri akış yönüne dik olarak etki eder ve ayırmada rol oynar. Kaldırma kuvvetleri parçacığa iki şekilde etki eder. Bunlardan biri kayma kaynaklı kaldırma kuvvetidir ve bu kuvvet parçacığı

merkezden duvara doğru iter. Diğer bir etki ise duvar kaynaklı kaldırma kuvvetidir ve bu kuvvet de parçacığı ters olarak merkeze doğru iter. Bu iki kuvvetin birbirine eşitlendiği noktada parçacıklar dengede kalmaya ve buna göre pozisyon almaya başlarlar. Bu düz kanallardaki dizilim prensibidir. Kanal tasarımına eğrisellik katıldığında parçacıkların ikincil bir kuvvete daha maruz kaldığı görülmüştür. Bu akış, akış yönü içerisinde merkez ve duvara yakın bölgelerde meydana gelen hız uyumsuzluğundan kaynaklanır. Eğrisel kanallarda kanal kesitinden bakıldığında alt ve üstte iki tane girdap oluştuğu görülür ve parçacıkların kesit boyunca dönme hareketi yapmasına neden olur. Bu kuvvete Dean kuvveti denir. Eğrisel kanallarda bu Dean kuvveti ve birincil kaldırma kuvvetlerinin bileşkesinin birbirine eşit olduğu yerde parçacıklar denge pozisyonu almaya başlarlar ve ayırma için gerekli olan dizilim başlamış olur. Burada önemli parametreler kanal boyutları, parçacık çapı ve uygulanan debidir. Dean kuvveti dolayısıyla eğrisel kanallar daha hızlı sonuç verir ve daha kısa kanallarla çalışılabilir.

Mikrokanalların üretimi genellikle soft litografi denilen teknik ile yapılır. Burada ışığa duyarlı polimer malzeme ile tasarılan şekil optik litografi yardımıyla Si- altlık üzerinde oluşturulur ve üzerine ana malzeme olan PDMS dökümü yapılır. Plazma işleminden sonra kanal cama yapıştırıldığında mikroçip üretilmiş olur. PDMS ucuz, toksik olmayan ve biyo-uyumlu olan bir malzemedir ve mikrokanal uygulamalarında geniş çapta kullanılmaktadır.

Bu çalışmada yaklaşık 15 mikron çapında olan MDA-MB-231 ve yaklaşık 20 micron çapında olan MCF7 insan meme kanseri hücreleri içeren karışımdan MCF7 konsantrasyonu için Dean akışından faydalanan dönele kanal tasarımı yapılmıştır ve buna göre yükseklik x genişlik 81 µm x 400 µm, 84 µm x 500 µm, 91 µm x 600 µm ve 86 µm x 700 µm olan kanallar üretilmiştir. Bu kanallar, bir giriş ve üç çıkışa sahiptirler. Her iki hücre kültür edildikten sonra hedef hücre olan MCF7 hücre iki farklı floresan boya ile boyanmış ve öncelikle bu boyaların hücrelerin yüzde kaçında etkili olduğunu belirlemek için akış sitometrisi ile analiz edilmiştir. Bu analizden sonra ilk önce uygun debileri bulmak için deney kurulmuş ve boyalı MCF7 hücreleri ve boyanmamış MDA-MB-231 hücreleri her birinden 100 ml’de bir milyon olacak şekilde toplam iki milyon hücre içeren karışım hazırlanmıştır. Bu karışımdan her bir kanal için 20’şer ml alınarak deneyler gerçekleştirilmiştir. Bu deneyler sırasında yüksek debilerde çalışılması gerektiği anlaşılmış ve ilk yapılan bu deneye göre gerekli debiye ulaşıldığında kanalların 2. çıkışlarında MCF7 hücreleri dizilimi olduğu görülmüş ve sonuçları doğrulamak adına akış sitometrisi analizi yapıldığında gerçekten de 2. çıkışlardan alınan MCF7 ışımaya yoğunluğunun diğer iki çıkışa oranla daha fazla olduğu görülmüştür. İkinci yapılan deneylerde MCF7 hücreleri ilkinden farklı bir boyayla boyanmıştır ve daha fazla sayıda debi incelenmiştir.

400 µm genişliğindeki kanalda yapılan deneyler sırasıyla 1000 – 1500 -1700 ve 2500 µl/dk debilerde gerçekleştirilmiş ve çıkışlardan her debi için ayrı ayrı işlemden geçen hücreler toplanmıştır. Dizilim görülen ve görülmeyen yerlerin fotoğrafları alınıp floresan yoğunluğu analizi yapıldığında dizilim olan – yeni başlayan ve dizilim görülen debiler belirlenmiştir. Buna göre yapılan akış sitometrisi analizleri de 1000 µl/dk debide MCF7 hücrelerinin her üç çıkışta bulunduğunu dolayısıyla zenginleştirme olmadığını ; 1500 µl/dk debide MCF7 hücrelerinin arka arkaya dizilmeye başladığı ve 1700 ve 2500 µl/dk debilerde ise çoğunluğu 2. çıkıştan toplanacak biçimde bir MCF7 zenginleştirilmesi elde edildiği görülmüştür.

500 µm genişliğindeki kanalda deneyler sırasıyla 1500 – 2000 – 2500 µl/dk debilerde gerçekleştirilmiş ve çıkışlardan her debi için ayrı ayrı işlemde geçen hücreler toplanmıştır. Dizilim görülen ve görülmeyen yerlerin fotoğrafları alınıp floresan yoğunluğu analizi yapıldığında dizilim olan – yeni başlayan ve dizilim görülen debiler belirlenmiştir. Buna göre yapılan akış sitometrisi analizleri de 1500 µl/dk debide MCF7 hücrelerinin her üç çıkışta bulunduğunu dolayısıyla zenginleştirme olmadığını ; 2000 µl/dk debide MCF7 hücrelerinin arka arkaya dizilmeye başladığı ve 2500 µl/dk debilerde ise çoğunluğu 2. çıkıştan toplanacak biçimde bir MCF7 zenginleştirilmesi elde edildiği görülmüştür.

600 µm genişliğindeki kanalda deneyler sırasıyla 2000 – 2500 – 3000 - 3500 µl/dk debilerde gerçekleştirilmiş ve çıkışlardan her debi için ayrı ayrı işlemde geçen hücreler toplanmıştır. Dizilim görülen ve görülmeyen yerlerin fotoğrafları alınıp floresan yoğunluğu analizi yapıldığında dizilim olan – yeni başlayan ve dizilim görülen debiler belirlenmiştir. Buna göre yapılan akış sitometrisi analizleri de 2000 µl/dk debide MCF7 hücrelerinin her üç çıkışta bulunduğunu dolayısıyla zenginleştirme olmadığını ; 2500 µl/dk debide MCF7 hücrelerinin arka arkaya dizilmeye başladığı ve 3000 - 3500 µl/dk debilerde ise çoğunluğu 2. çıkıştan toplanacak biçimde bir MCF7 zenginleştirilmesi elde edildiği görülmüştür.

700 µm genişliğindeki kanalda deneyler sırasıyla 2500 – 3000 - 3500 µl/dk debilerde gerçekleştirilmiş ve çıkışlardan her debi için ayrı ayrı işlemde geçen hücreler toplanmıştır. Bu debilerin hiçbirinde istenilen dizilim görülememiş ve floresan yoğunluğu analizleri de bunu doğrulamıştır. Buna göre yapılan akış sitometrisi analizleri de 700 µm genişliğindeki kanalda MCF7 hücrelerinin her üç çıkışta olduğunu ve buna göre zenginleştirme elde edilemediğini göstermiştir. Bu kanalda dizilim sağlamak için 3500 µl/dk'dan daha yüksek debilerde çalışılması gerektiği görülmüş ancak şırınga pompasının 3500 µl/dk'dan yüksek debilerde etkin çalışmaması dolayısıyla bu deney gerçekleştirilmemiştir.

Bu tez kapsamında üretilen dönele kanallar, uygun debilerde çalışıldığında tasarımlarına uygun olarak hedef hücrenin tek çıkıştan toplanabilmesini sağlayarak zenginleştirme vermiştir. Böylece aynı soydan iki farklı hücre tipinden biri diğerinin içinde zenginleştirilip uygun analizler sonucu ayırt edilebilmiştir. Yüksek debilerde çalışıldığı için deney süresi 10 dk'nın altındadır ve böylece hızlı sonuç alınabilmiştir. Tüm bunlara ve maliyetinin de düşük olması sebebiyle üretilen dönele kanallar, ucuz ve küçük boyutlu hızlı ve daha doğru sonuç alınabilecek bir teşhis cihazı geliştirmede ön çalışma olarak kullanılabilecek bir tasarım olmuştur.

1. INTRODUCTION

The word microfluidics simply refers to pass a fluid that has very small volume through a device having channels or cubicles. They are commonly used for performing in vitro tests as many conventional cell analysis systems. They can also be used for biochemical molecule processing and delivery systems. Interaction between materials and devices and systems that has been developed can be seen in Fig.1.1. Microfluidic chips have advantage over conventional in vitro techniques that are commonly used since they allow controlling the medium for every single cell. There are no unwanted factors, diffusion and different cell populations and the reagents for cells are controlled [1].

There are so many studies about cancer but low survival rate and malignancy remains complex [2]. Using microsystems will provide detection of cells which have quite heterogeneous forms like cancer individually, and will lead to study many diseases and understanding of their mechanism [3]. Most of the microfabricated technology such as DNA microarray gives the result of a snapshot instead of giving real-time monitoring. However, real-time monitoring is so important to investigate the malignant tumors that have highly dynamic structure depending on their adjustment with the medium in which they are living.

Producing anticancer drugs and new POC (point-of care) devices will be pioneered by increasing knowledge of how malignant tumors reacts to treatment, their resistance and molecular morphology. Microfluidic LOC (Lab-on-a chip) and μ TAS (micro-total-analysis-systems) technologies are promising areas since they provide analysis of single cells even though complexity of cells is very high [2].

Microfluidics has been becoming widely used in molecular and cellular biology. Microfluidic chips provide fast and exact diagnosis due to their realibility and controllable capabilities. Miniaturizing provides us many advantages in diagnostic device such as use of small amount of samples, fast reaction time, and different types of tests in one chip and cheapness [4].

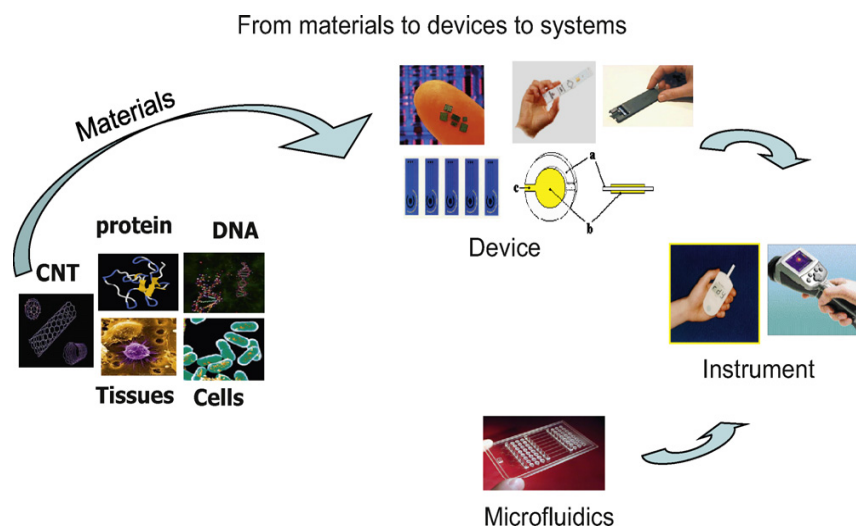


Figure 1. 1 : Interactions between techniques and materials [5].

1.1 Literature Review

Cancerous media is a molecular structure that is continuously evolving due to cell interaction, and they are heterogenic. Microfluidics has found many application areas such as cancer diagnostics and monitoring for various different cell types.

There are active and passive sorting methods with using microfluidic channels. Active systems use the advantage of external stimulus such as electric field (DEP-dielectrophoresis), acoustic forces (acoustophoresis), and optics (optical tweezers) [6], magnetic field (magnetophoresis) [7]. Although efficiencies of these techniques are high, they have limitations due to requirement of expensive equipment such as AC or DC power supply or lasers. Passive sorting techniques do not need any external force to manipulate cells or particles. This makes them more cost-effective and miniaturized devices.

Studies had been made in microfluidics were done by blood decomposition, especially white blood cells. Sethu et al. developed a microfluidic device for diminishing white blood cells (WBCs). In their system while red blood cells (RBCs) were passing through and leaving the system, WBCs were remained. They put filtration elements on the sides of the channel to prevent clogging instead of collectting RBCs. They designed expanding geometry to get equivalent volumetric flow rate. They accomplished 97% decomposition with this diffusive technique [8].

Ji et al. demonstrated that pillar filters and cross-flow filters has high WBC depletion and they can be used in large volume of samples [9].

Hosokawa et al. developed microcavity array for sorting lung carcinoma cell depending on size and deformability. They used negative-pressure to lead the cell suspension through the arrays. They captured the cells with 97% efficiency and 98% viability. They used this technique in various cell types like breast, colon and gastric tumor cells with higher than 80% efficiency [10].

VanDelinder et al. searched for usage of cross-flow filters and they found that RBC clogging is an obstacle. They used repeating microfluidic array geometries and they were succesful at 98% WBC sorting without RBC lysis [11].

Davis et al. used microfluidic devices with pillars which was shown in Fig. 1.2. They used this micropillar to get particle sized pathline. By this way, they sorted the pre-determined target cells just depend on size. They depleted lymphocytes with 100% efficiency [12].

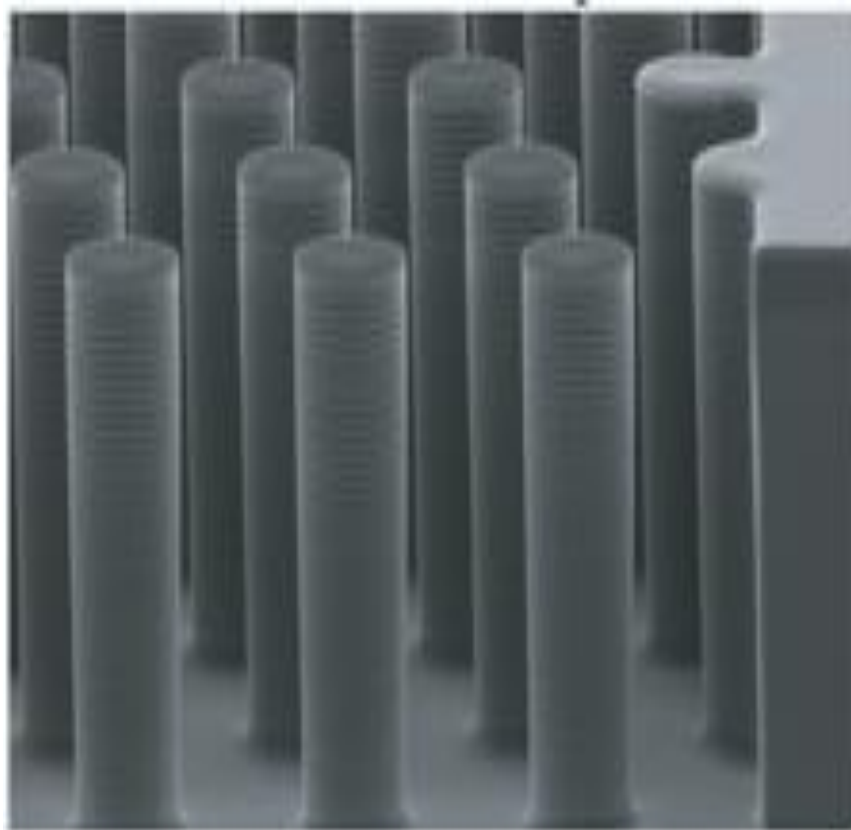


Figure 1.2 : SEM image of pillars [12].

Zheng et al. developed parylene microfilters as in Fig. 1.3. to isolate the immortalized prostate cancer cell lines. They used pressure-driven flow to get

through the suspension from microfilter and they recover cells at 90% efficiency [13].

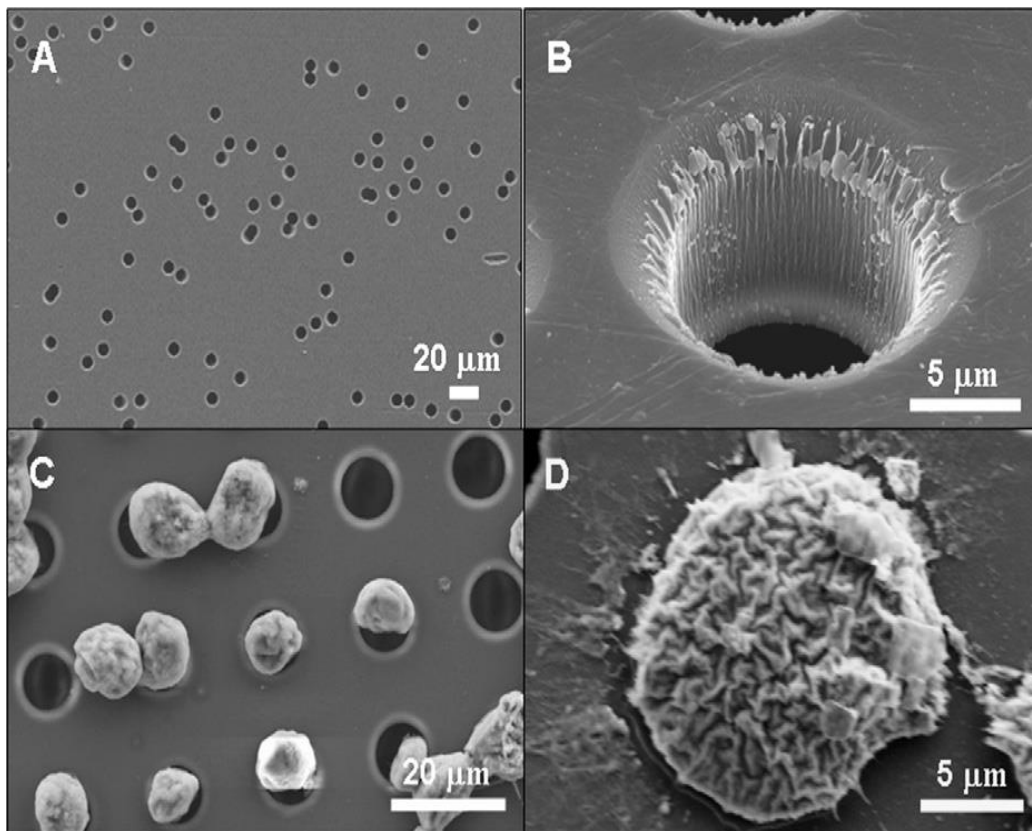


Figure 1.3 : SEM images A) Commercial pored membrane B) Parylene filter C-D) Captured cells [13].

Chen et al. wanted to isolate the cancer cells based on their deformability. So that, they combined experimental results and physical modeling. They used a filter especially fabricated for model lung adenocarcinoma cells. They captured the cells with 99,9% efficiency from diluted human blood samples. Sheat flow took advantage of low Reynolds number of the fluid. This is related to use certain geometries or different flow rates of parallel fluids. Against size-based sorting this only applies fluid stress but suspensions which are dense must be diluted [14].

SooHoo et al. used aqueous two-phase system based on microfluidics for enrichment of leukocytes in blood suspension. They achieved 100% RBC depletion [15].

Zheng et al. used T shaped channels and separated WBCs from RBCs. By setting T channel's length and side walls between upstream and downstream, cells went different flow ways just based on the size and working principle was demonstrated in Fig.1.4. WBCs from diluted blood with 97% efficiency were separated in their

research. They also found that separation WBCs from RBCs was influenced by RBC orientation [16].

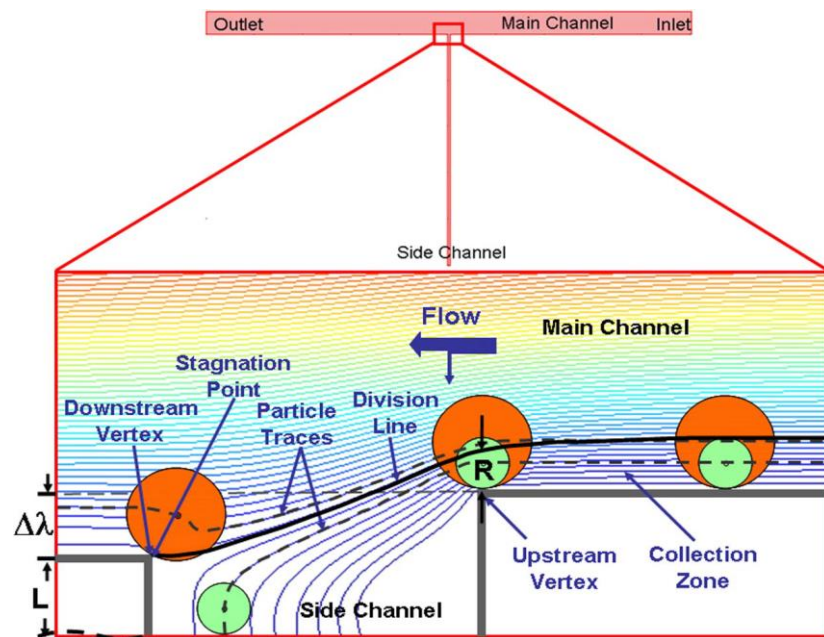


Figure 1.4 : Separation principle of device [16].

Kuntaegowdanahalli et al. used spiral microchannels. They used five loop archimedean spiral microchannel. As shown in Fig. 1.5 (a) they showed separation of 10, 15, and 20 μm polystyrene particles from each three outlets out of eight, individually. Then they used this method to separate neuroblastoma cells from glioma cells. Collected cells from each outlet were shown in Fig. 1.5 (a). They yield 80% separation efficiency and they put cells in culture again and they exhibit 90% viability [17].

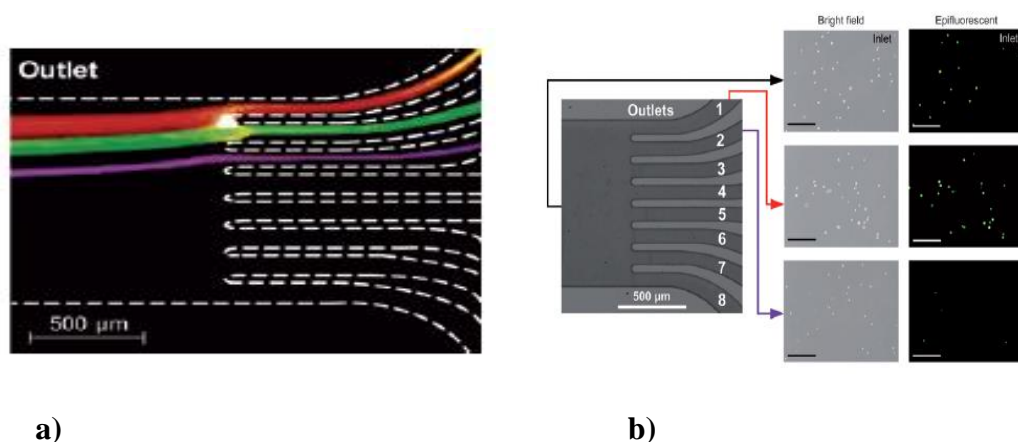


Figure 1.5 : (a) : Particle experiment (b) Cell experiment [17].

Du et al. showed enrichment and capture of cervical cancer cells in microfluidic channel. Tumor cells were captured efficiently and they found that capture rate and efficiency rate were depend on flow rate and antibody concentration which was used for treating channel [18].

Kwon et al. used adhesion difference for breast cancer cells and they used microfluidic device to separate them without labeling. As shown in Fig. 1.6 they put three types of nanostructures into the microfluidic channel. They did not have bad effect on flow conditions. They used MCF10A (human breast epithelial cells) and MCF7 (breast carcinoma cells). According to the results MCF 10A cells were more sensitive to surface topography than MCF 7 cells. They saw that MCF 10A had more adhesion strength than MCF7 [19].

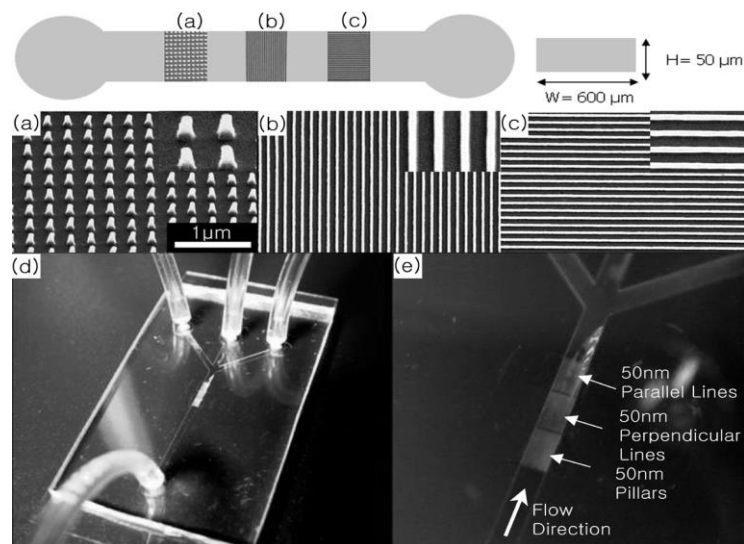


Figure 1.6 : SEM images of microfluidic device a) 50 nm pillars b) 50 nm perpendicular lines c) 50 nm parallel lines d) image of microfluidic channel e) image of nanopatterned region [19].

He et al. designed a microfluidic device to investigate cancer cell from body fluid. They used mixtures of MCF 7 and MCF 10A cells. They were captured by serpentine weir filters. After 4 min. contact, MCF 7 could be detected by a selective fluorescent complex. The signals they get were seven times stronger than doing these procedures on conventional glass slides [20].

Within SmartHEALTH project, so many microfluidic device were examined. They were related to plasma preparation unit, mixing element and assay enhancement platforms. They worked not only detection of different samples, also different sensor technologies. SmartHEALTH's next projects will be interested in combination of

several functional elements (nucleic acids, RNA marker for cancer detection) and also RT-PCR applications [21].

Kim et al. acquired simple and robust interface between human breast cell and device. They did not just implement thin section tissues to the chip, they also had perfect fluid control without cross-contamination, bubble production, and leakage for different solutions as well. They examined four different biomarkers on breast cancer cells. Their results showed that several cancer proteins on a tumor section can be investigated simultaneously [22].

Multiple myeloma is an immune system cancer. It consists of plasma cells which are named as monoclonal B and IgH VDJ gene and it is characterized by these unique molecular signature. Pilarski et al. demonstrated usage of capillary electrophoresis for detection of PCR (polymerase chain reaction) product which has amplified from genomic DNA and transcription from a patient who had myeloma. IgH VDJ transcripts were at high abundance whereas DNA was at low abundance. They used an integrated PCR system which contained cell processing, PCR and RT-PCR (reverse transcription) at the same time. According to them microfluidic system in their study will improve the portable diagnosis, provide high access with low costs and diagnosis devices providing more sophisticated clinical test will be developed [23].

Geometry of microfluidic channel is important in detection sensitivity. Bang et al. used flow focusing channel to reduce the complication of channel geometry and they obtained high sensitivity detection and throughput. The channel width was 100 μm at inlet and 500 μm at detection side. Fluorescently labelled particles were hydrodynamically focused and passed through from the expansion region to detection region. They obtained higher sensitivity when it is compared to normal channels because of reduced flow velocity at detection zone in the expansion channel [24].

Liu et al. made a microfluidic cartridge to study gene expression of human leukemia. They studied human neck and head cancers using oral fluids. Into the microfluidic device there inserted antibody conjugated with magnetic beads and they assisted in removal of all lymphocyte cells. They captured and enriched the primer cancer and

cancer cells with antibodies and surface glycolproteins for expression. The cancer cells was isolated and detected [25].

Lien at al. isolated and detected cancer cells from large sample of volume using microfluidic channel containing antibody coated surface with surface modified magnetic beads. According to their results 90% of the target cancer cells were isolated [26].

Chikkaveeraiah et al. manufactured a microfluidic system to find protein cancer biomarkers. They used heavily-enzyme-labeled superparamagnetic particle-antibody bioconjugate and they measured PSA (prostate specific antigen) and interleukin-6 (IL-6) biomarkers in prostate cancer serum after 1,5 hours assay time. Results were perfectly relevant with standard enzyme linked immunosorbent assay [7].

Salibaa et al. used cell sorting method with biofunctionalized microfluidic channel containing self-assembled superparamagnetic beads. They called this device as ‘*Ephesia*’. Microfluidic device has combined the advantage of particle sorting (flow-activated interaction) and immunomagnetic sorting (use of batch-prepared, well characterized antibody bearing beads) as shown in Fig. 1.7. Their yield was better than 94% capture [27].

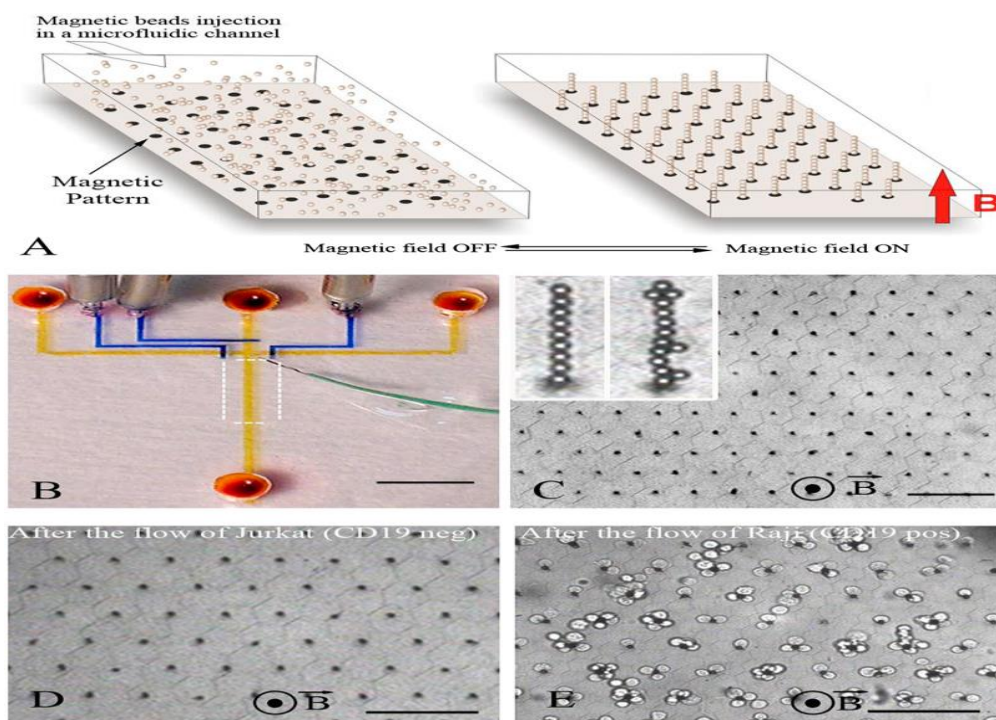


Figure 1. 7 : A) Principle of device B) PDMS microchip C) Magnetically assembled array D) Jurkat cells E) Raji cells [27].

Nagrath et al. used biofunctionalized arrays of pillars and they captured CTC (circulating tumor cell) from the patients' blood containing different types of cancer as shown in Fig.1.8. Efficiency of the system was high. However, this system requires direct modification on the surface of pillar for each chip. Absence of antibodies and thick and opaque pillars requires specific software and limits the characterization of captured cells optically[28].

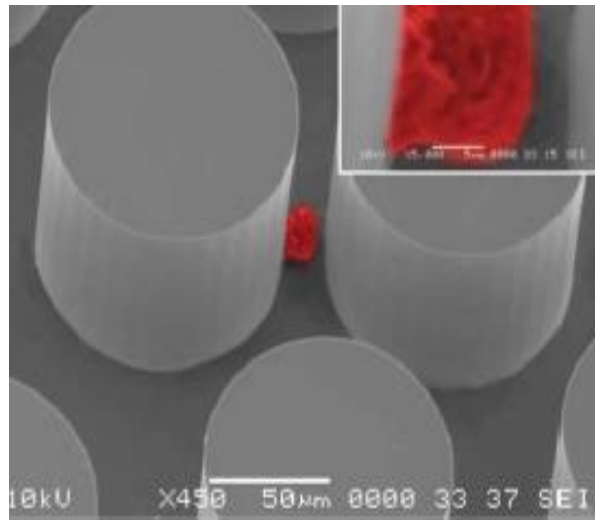


Figure 1.8 : Image of captured lung cancer cells from blood [28].

2. THEORY

2.1 Inertial Microfluidics

When neutrally buoyant particles in a suspension are passed through a microchannel they experience both viscous and drag forces without any external force. Location of the particles in a carrier fluid is primarily determined by drag forces. Inertial lift forces are responsible for the motion of particles along the channel and shear induced inertial lift forces arise as a result of parabolic profile of Poiseuille flow velocity (F_{Shear}) and these particles which experience this force are tend to migrate towards the wall from the channel center. As shown in Fig.2.1 while particles are moving towards the wall, they experience a second force which is called wall effect (F_{Wall}) and this force pushes the particles towards to center. F_{IL} and F_{WL} effects the particles in the flow at opposite direction [29]. Particle diameter to channel hydraulic diameter ratio (a_p/D_h) has important influence over these forces and *Segre and Silderberg* showed that when $a_p/D_h \geq 0,07$, particles can equilibrate $0,2D$ away from the channel wall [30]. Larger particles experience higher shear rate and a_p/D_h values for these particles are higher, thus particles are pushed away form the center towards the surface particles away from the center towards to surface. Furthermore, as the velocity of a fluid in a tube increases, equilibrium positions shift to the wall [30].

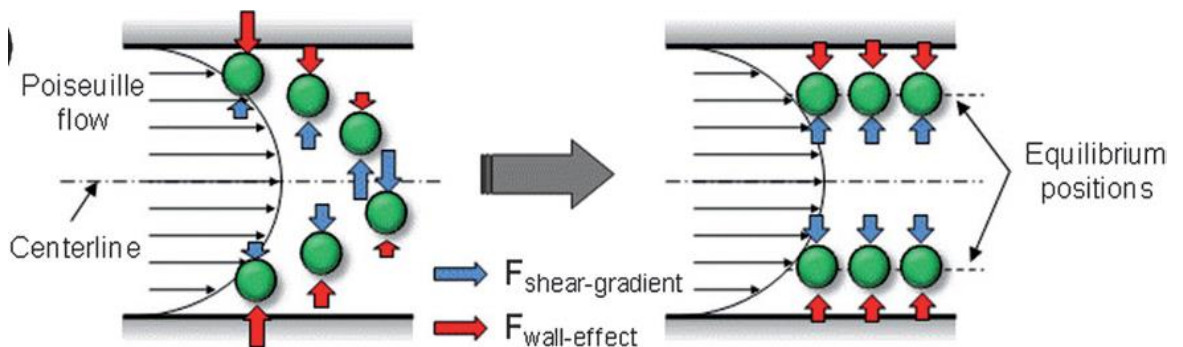


Figure 2.1 : F_{Wall} and F_{Shear} effects [31].

Viscous drag force and net lift forces are two main forces that acts on particles in a microchannel. Viscous drag force is described as

$$F_{\text{Drag}} = 3\mu\pi a_p U_f \quad (1.1)$$

and a_p is particle diameter, μ is fluid viscosity, U_f is average fluid velocity. According to this formula, drag forces depend on particle diameter and fluid velocity. *Asmolov* approximately calculated the lift force acting on a particle in Poiseuille flow as

$$F_L = \rho G^2 C_L a_p^4 \quad (1.2)$$

where ρ is fluid density, G is shear rate which is $G = 2U_f/D_h$, $D_h = 4\text{Area}/\text{Perimeter}$ and C_L is lift coefficient. Although *Asmolov* derived that C_L differentiates with Reynold's number, generally it can be estimated as $\sim 0,5$ in microfluidic applications [32]. C_L is a function of distance and it is a sign to existence of lift forces in environment. According to this, a positive C_L value means that the particle migrates away from the wall while a negative C_L value indicates that the particles approaches to wall than center. If the net lift force acting on a particle is rewritten as [29]

$$F_L = \frac{2\rho U_f^2 a_p^4}{D_h} \quad (1.3)$$

2.2 Dean Secondary Flow

The mismatch between downstream direction and velocity that manifests at the curved channel center and wall generate a secondary flow. Therefore, the inertia that channel centered particles have is greater than the ones close to channel wall and they tend to form outward flow across the curve. Pressure gradient forms along the channel radial direction. Since the channel is closed, relatively stable fluid turns inward again and generates two symmetrical vortices when it is observed from the channel cross-section due to centrifugal acceleration in curvilinear channels. They are at opposite direction and positioned at upper and lower sections of the channel as shown in Fig.2.2 [33].

Magnitude of these vortices are determined by a dimensionless number called Dean number and it is expressed as

$$D_e = \frac{\rho U_f D_h}{\mu} \sqrt{\frac{D_h}{2R}} = Re \sqrt{\frac{D_h}{2R}} \quad (1.4)$$

where R is the Radius of curvature Re is fluid Reynold's number.

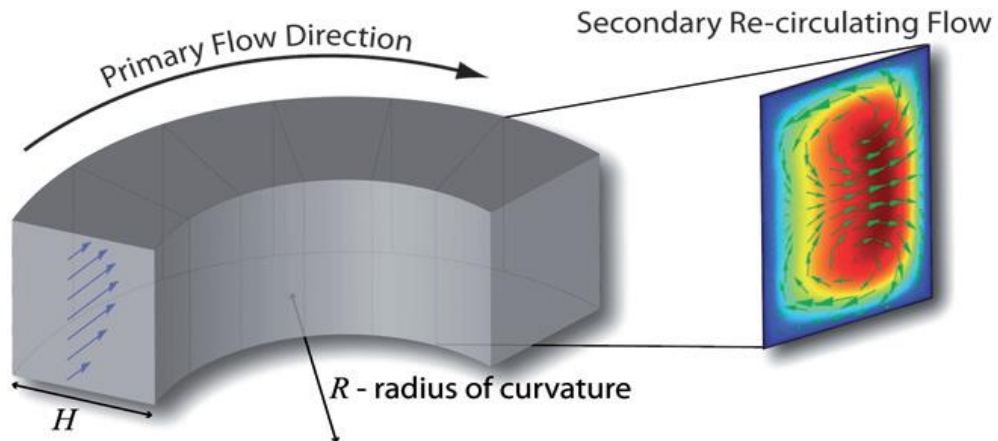


Figure 2.2 : Dean flow in curved channels [34].

In straight channels $D_e = 0$ because there is no curvature in these kind of channels. $R=0$, so Dean flow does not manifest itself in these channels. In other words if the radius of curvature decreases, magnitude of Dean vortices increases. Fig. 2.3 shows that particles in curvilinear experience both Dean force (F_D) and net lift force (F_L) which is combination of shear induced lift force (F_{Shear}) and wall induced lift force (F_{Wall}). Shear force drags the particle, the particles outside of the center because of the parabolic nature of Poiseuille flow. Wall effects push the particles away from the wall to the center [34].

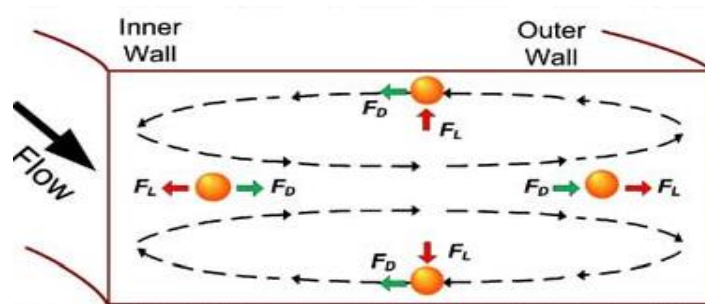


Figure 2.3 : Forces acting on a particle in curved channels [35].

Balance between these two forces makes the particles to be positioned at four equilibrium sites in rectangular cross-sectioned channels at low Reynold's numbers.

Dean secondary flow and inertial lift forces act on a particle in a fluid flow at superposition. At an inertial equilibrium position, drag force acts on a particle which is kept stationary. This Dean force is perpendicular to the primary flow direction and then will compete with inertial lift force and capture the particles in this secondary

flow and tend them to equilibrate. For focusing and filtration applications, less number equilibrium positions resulted from Dean secondary flow demonstrated in square and near square cross-sectioned channels. It is observed that adding curvatures to channels has advantageous due to migration of equilibrium positions away from the channel center, shorter channel lengths and allowing separations because of different F_L/F_D values to each particle size.

In curved channels $a_p/D_h > 0,07$ particles are exposed to both inertial lift force and secondary Dean flow. Combination of these forces provide accurate focusing of particles in separation and concentration applications. When Dean force which arises in curvilinear channels is added, the positions reduces to single position in internal channel wall due to combination of net lift force and Dean force.

Magnitude of Dean vortices increase with incremental fluid velocity as a result of higher centrifugal forces acting on particles. Average Dean velocity is expressed by Ookawara et al. as

$$\bar{U}_{Dean} = 1,8 \times 10^{-4} D_e^{1,63} \quad (1.5)$$

for a known Dean number [36].

These two opposite directioned vortices which force particles to follow fluid movement are depend on particle diameter. According to this, Dean force is expressed as [35]

$$F_D = 3\mu\pi\bar{U}_{Dean}a_p = 5,4 \times 10^{-4} \mu\pi D_e^{1,63} a_p \quad (1.6)$$

Curved channels designed to focus 20 μm diameter cells in thesis and key design criteria were $a_p/D_h > 0.07$, $F_L/F_D \geq 1$.

3. MATERIALS AND METHOD

3.1 Fabrication of the Microfluidic Device

3.1.1 SU-8 photoresist

SU-8 3050 was used in fabrication process and purchased from MicroChem Company. It is an epoxy-based photoresist that gives stable structure under any physical or chemical conditions. 3050 means that if the spinning speed is 3000 rpm, final coating thickness will be 50 microns which is mentioned in SU-8 3000 datasheet provided from MicroChem Company. SU-8 is a negative photoresist which gets harden and insoluble after UV exposure. Hence the mask should be designed and published suitably for response of the photoresist to UV exposure [37].

3.1.2 Acetate mask fabrication

Acetate masks were used due to their low cost and efficiency for desirable pattern. After determining the channel dimensions and shapes that were suitable for design criteria, they were drawn via Tanner Tools L-Edit 1.3.0 and published in acetate. Since SU-8 is a negative photoresist, the regions where the channel pattern is located in the mask was transparent and must be harden after UV exposure. Because of that rest of the mask was published in dark as shown in Fig 3.1.

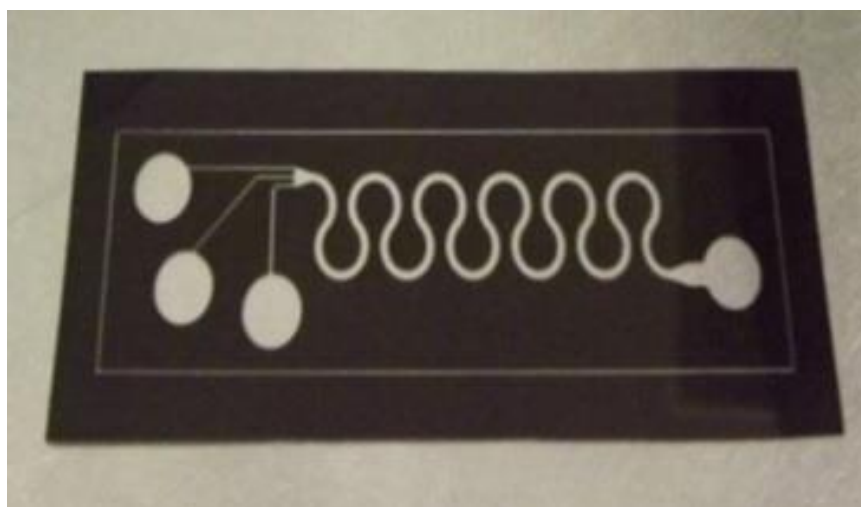


Figure 3. 1 : Acetate Mask.

3.1.3 Fabrication of master mold

Laurell WS 400 B Spinner was used to coat SU-8 photoresist onto Si-wafer to get homogeneous coating and desired thickness in short time. Locating the wafer onto spinner properly was highly critical to get homogeneous coating on the surface. Since the working principle of spinner is centrifugal force, locating the wafer evenly and pouring SU-8 exactly in the center of the wafer are important. After wafer was located and SU-8 was poured, appropriate program is adjusted to get desired thickness coating. Fig. 3.2 shows how film thickness is changing with spin speed for different version of photoresist.

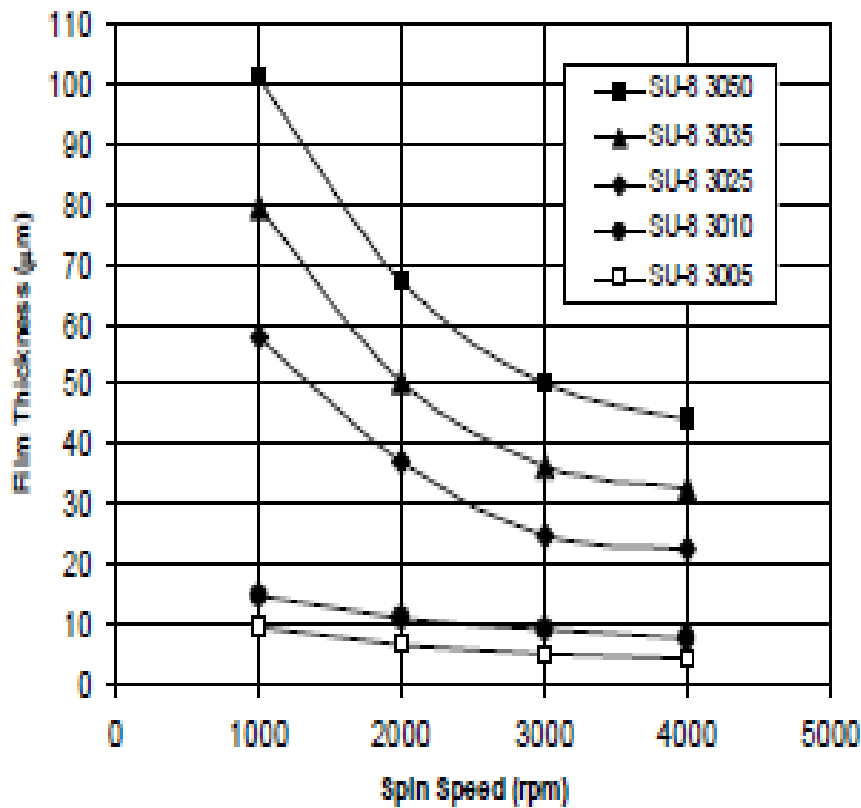


Figure 3.2 : Thickness vs Spin Speed (21°C). [37]

After spin coating step, Si-wafer was put onto 95°C PRAZITHERM hot plate for 40 min. to constitute mechanical stability and adhesion between wafer and SU-8 photoresist. This process was called as soft bake. Time durations for varied thickness values were mentioned in SU-3000 datasheet. Used soft bake times, exposure energy and thickness can be found in Table 3.1 and Table 3.2 for 80 – 100 µm thickness.

Table 3.1 : Soft Bake Times.[37]

Thickness (μm)	Soft Bake Time
4 - 10	2 – 3
8 - 15	5 - 10
20 - 50	10 - 15
30 - 80	10 - 30
40 - 100	15 - 45

After soft bake, the pattern is produced on photoresist via OAI Model 200 Mask Aligner.

Table 3.2 : Thickness and Exposure Energy.[37]

Thickness (μm)	Exposure Energy (mJ/cm^2)
4 - 10	100 - 200
8 - 15	125 – 200
20 - 50	150 – 250
30 - 80	150 – 250
40 - 100	150 – 250

Wafer was placed onto mask aligner plate and masks were placed on wafer and then pushed under UV light for 8 min. Since optimum exposure time for 20-100 microns thickness, photoresist coating was 8 sec. according to SU-8 3000 datasheet. Post exposure bake time was 1 min. on 65°C hot plate and 95°C for 3-5 min. In Table 3.3 and Table 3.4, post exposure bake times and development times were presented.

Developer stage takes place after UV exposure and post exposure bake steps to dissolve the soluble parts because the exposed parts were solidified. After developing for 15 min. the desired pattern was created onto the wafer and the patterned wafer was washed with SU-8 developer, isopropyl alcohol and DI water; dried with

nitrogen. After all the processes were hard bake process took place to get thermally, physically and chemically stable mold for at least 2 hours.

Table 3. 3 : Post Exposure Bake Times.[37]

Thickness (μm)	PEB Time 65°C (min)	PEB Time 95°C (min)
4 – 10	1	1 - 2
8 – 15	1	2 – 4
20 – 50	1	3 - 5
30 - 80	1	3 – 5
40 - 100	1	3 - 5

Table 3. 4 : Development Times.[37]

Thickness (μm)	Development Time (min)
4 -10	1 - 3
8 - 15	4 – 6
20 - 50	5 – 8
30 - 80	6 – 12
40 - 100	7 - 15

3.2 Channel Fabrication

Soft lithography has been used extensively in fabrication of microfluidics systems. The details of fabrication scheme are schematically described in Fig. 3.3. Basically, it is composed of six steps with a start of bare-Si and ending up with fully functional microfluidic system. Among the fabrication steps, PDMS casting and O₂-plasma treatment are two the most critical ones as described below.

3.2.1 PDMS casting

PDMS (polydimethylsiloxane) is widely used for biomems applications due to its unique properties. PDMS is nontoxic, transparent material and can be cured at low temperatures. It is easy to mold and that makes it great candidate to be used in soft

lithography techniques. PDMS is an elastomeric polymer and since it has high flexibility and it can be peeled from the master mold without getting damage [38].

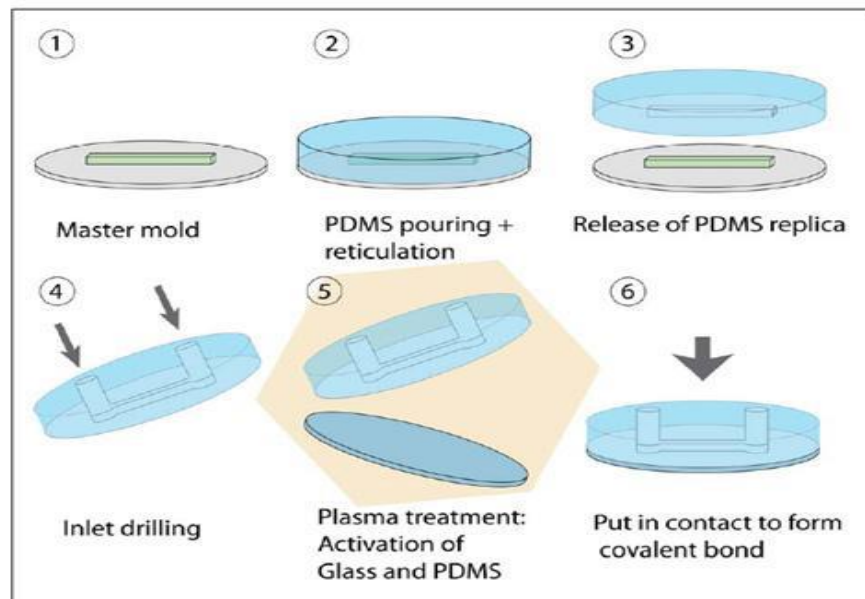


Figure 3. 3 : Schematic illustration of PDMS channel production. [41]

PDMS Sylgard 184 was purchased from Dow Corning Co. used for casting material as well. A petri dish was coated with aluminium foil and SU-8 master wafer was stuck to this petri dish with double-sided tape to avoid leakage of PDMS under wafer. PDMS and its curing agent was mixed at 10:1 and stirred until a homogeneous mixture was obtained. Then the mixture was poured onto SU-8 master and then put in degassing oven for dissipating air bubbles from PDMS. When the degassing was over it was put into 75°C oven overnight to get solid rubber.

Solid PDMS was peeled from the master carefully and master can be used for other channel fabrications if it is not damaged. The part of the PDMS where the channel was located was cut with scalpel and outlets were drilled with 0.5 mm cutting core.

3.2.2 O₂ plasma treatment

Since PDMS is hydrophobic it is hard to wet and can not adhere to a surface easily [38]. surface modification is needed to achieve these objectives. Harrick Plasma device was used in this work. First PDMS channels and glass microslides were cleaned with isopropyl alcohol, DI water and dried with nitrogen and put onto 40°C hot plate for 15 min. to dry them completely. Then they were put onto plasma device

on a plate. They were exposed to medium RF level O₂ plasma for 40 sec. and they stucked together and put onto 75°C plate to improve adhesion.

High RF power and long exposure times create a brittle silica layer and that causes cracking but at lower RF levels and short exposure times cracking can be avoided and a suitable oxidized layer can be obtained. That is important for improving the surface to surface adhesion between PDMS and glass microslide [40].

3.3 Experimental

3.3.1 Depth analysis

One of the critical parameters of channel design is channel depth – height (H)- and it is crucial for working mechanism of the microfluidic device. These parameters and surface roughness as well were analysed with Ambious XP 300 Plus Series Profilometer. Fig. 3.4 shows a profilometer data example. Profilometer has diamond single crystal cantilever to detect two successive peaks and dips. It gives information about channel height and surface structure after measuring at least three times from different regions of the wafer.

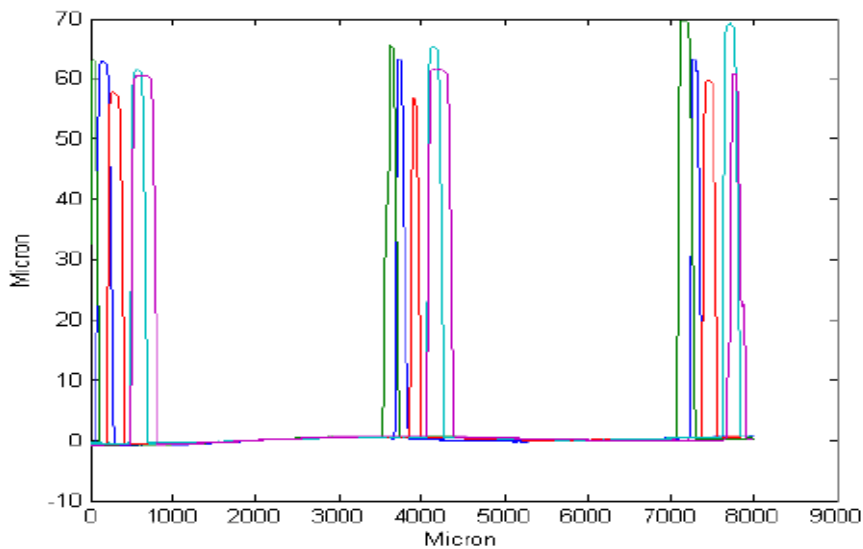


Figure 3. 4 : Profilometer analysis result.

3.3.2 Optical microscope analysis

Since any distortion on SU-8 master will effect the formation PDMS, it is important to characterize the channel with optical microscope to prevent using a defected channel that may disrupt the flow profile. Olympus optical microscope was used to

detect defects from fabrication process and any contamination that might have caused by several environmental reasons such as dust and water residues.



Figure 3.5 : Optical microscope image of a defected channel.

3.3.3 Design

Channels were designed to focus cells which have nominal 20 micron diameter and SU-8 masters for $W = 400, 500, 600, 700 \mu\text{m}$ wide channels were fabricated. Focusing particles at one direction is important in particle or cell sorting experiments. Curved channels were used to focus MCF7 human breast cancer cells which have approximately 20 micron diameter in rectangular cross-sectioned microchannels. Effects of flow rate on cell focusing were investigated in curved channels which have one inlet and three outlets as shown in Fig. 3.6.

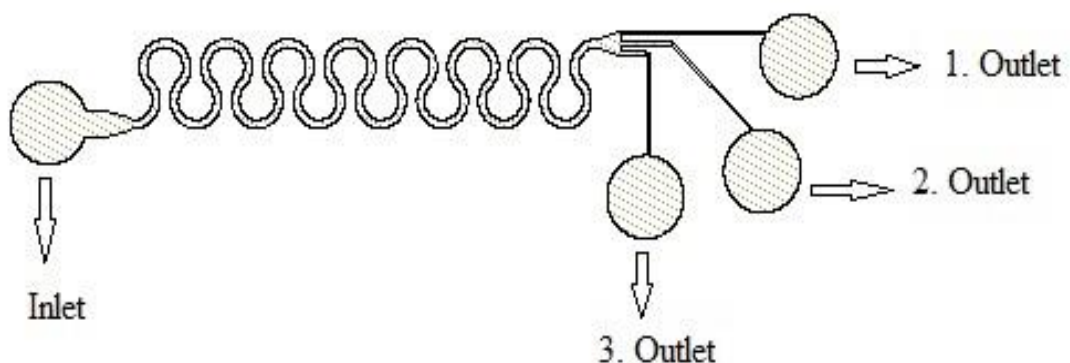


Figure 3. 6 : Channel design and outlet positions.

Channel dimensions was given in Table 3.5 and microscope image of channel outlets was given in Fig. 3.7.

Table 3. 5 : Channel Height – Channel Width Table.

Height (μm)	Width (μm)
81	400
84	500
91	600
86	700

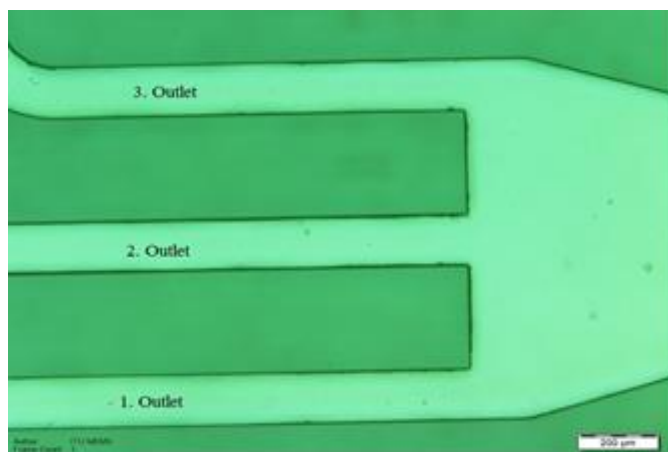


Figure 3. 7 : Channel outlet positions in microscope image.

Theoretical parameters for each channel dimensions due to flow rates were given in Table. 3.6.

Table 3. 6 : Focus Parameters According to Theoretical Calculations

Width (μm)	$a_p/D_h \geq 0.07$	Flow Rate ($\mu\text{l}/\text{min}$)	$F_L/F_D \geq 1$
400	0.14	1700	1.98
400	0.14	2500	2.29
500	0.13	2500	1.73
600	0.12	3000	1.33
600	0.12	3500	1.40
700	0.13	3500	1.81

3.3.4 Flow cytometer

Flow cytometry was used for counting, sorting cells and detect biomarkers form a suspension which takes advantage of laser based technology.

Working principle is based on sending a laser light beam to the cells in a suspension and detect the scattered light from each cell also fluorescent light from cells which are fluorescently labeled with one or more detectors and they are excited with the incident laser beam and yield longer wavelength emission peaks as shown in Fig. 3.8. Combination of these data gives the information about cells. Forward Scatter roughly corresponds the size of the cell while Side Scatter is related with inner complexity [42].

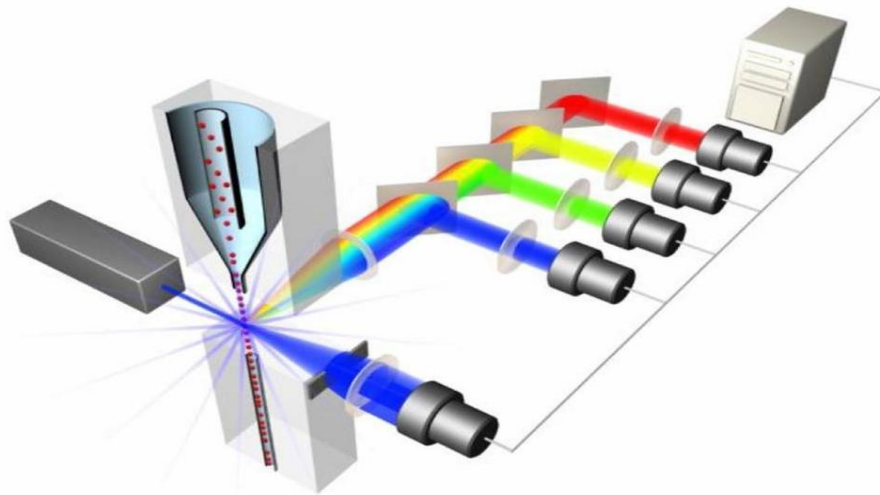


Figure 3. 8 : Flow Cytometry Mechanism. [43]

Fig. 3.9 shows a flow cytometer data of fluorescently labeled MCF7 cells. Right window shows live and fluorescently labeled cell while left window indicates unlabeled and/or dead cells. Right window was considered as interrogation region for reading data.

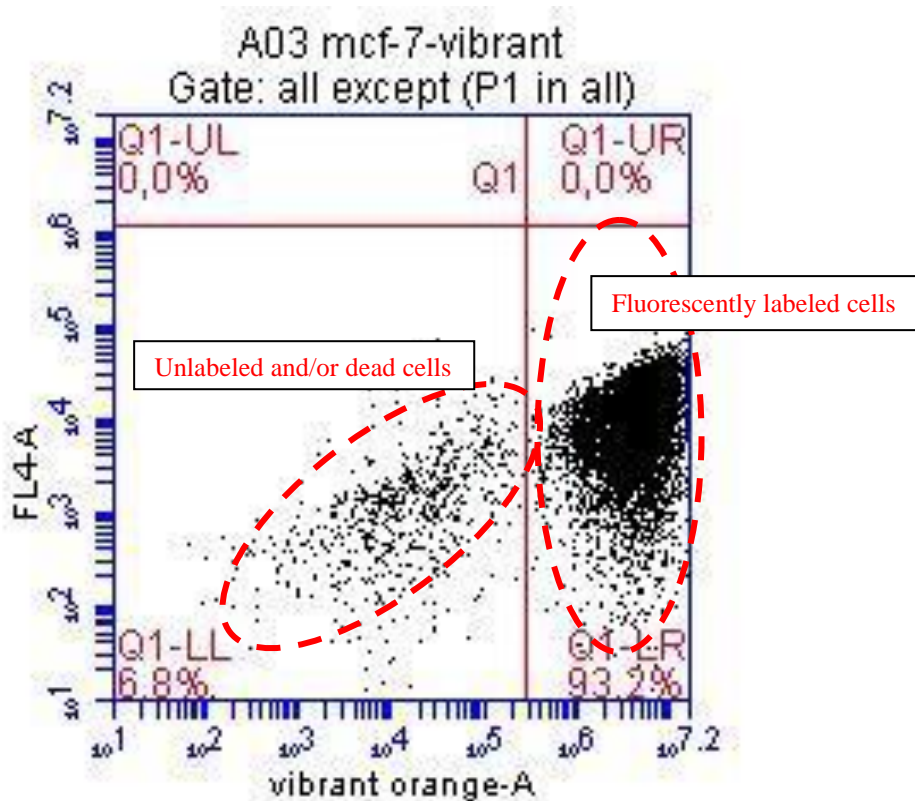


Figure 3. 9 : Flow Cytometer Data.

3.3.5 Cell mixture

MCF7 and MDA-MB-231 breast cancer cell lines which have approximately 20 μm , 15 μm diameter respectively were used. They were obtained from DETAE, Çapa Medical School and cultured in MOBGAM, ITU. Vybrant DyeCycle Orange fluorochrome was used for flow cytometry and optical microscope analysis were done for determining the required flow rates. It had an excitation peak at 519 nm and emission peak at 563 nm which yields reddish - orange colour. CFSE (Carboxyfluorescein Succinimidyl Ester) was used at second experimental setup. It had an excitation peak at 494 nm and emission peak at 521 nm which yields green colour. MCF7 cells the target cells which means curved channels that are used in this thesis were designed to focus MCF7 cells. They were first labeled with Vybrant DyeCycle Orange and CFSE while MDA-MB-231 cells were unlabeled. This mixture were passed through the channels at various flow rates to observe focus positions of MCF7.

Fluorescently labeled MCF7 cells analyzed with flow cytometer to determine the effectiveness of dyes. Cell mixture was analyzed before enrichment procedure with flow cytometer to determine fluorescence percentage at the beginning.

Two different fluorescence dyes used in experiments Fig. 3.10 shows how much of the MCF7 cells are dyed with Vybrant DyeCycle Orange in first experiment and with CFSE in second experiment as first and second group. According to these results Vybrant DyeCycle Orange dyed 93.2 % of MCF7 cells and CFSE dyed 93.3 % but at second group cell mixture CFSE dyed 84.6 % of MCF7 cells. Thus CFSE dyeing efficiency was lower at second group of cells. Initial MCF7 majority was analyzed with flow cytometer and Fig. 3.11 shows the MCF7 population percentages from MDA-MB-231 – MCF7 cell mixture before passing them through the channels. Cell mixture contains 1 million MCF7 and 1 million MDA-MB-231 cells in 100 ml PBS. Experiments were done with 20 ml syringe, that means there were 20.000 cells/ml for each channel.

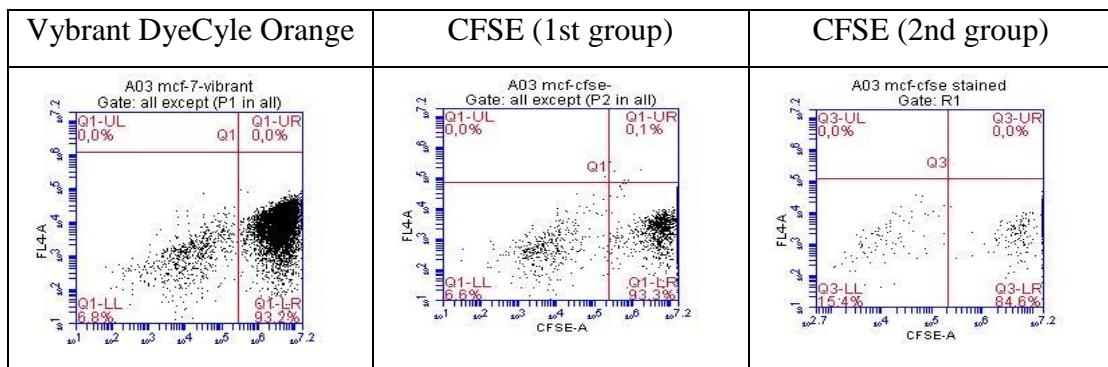


Figure 3. 10 : Fluorescent dye efficiencies.

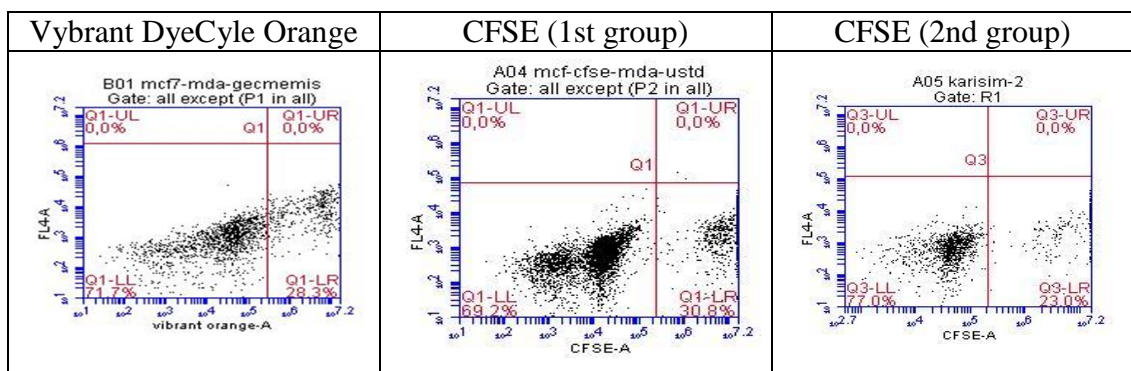


Figure 3. 11 : Cell mixture flow cytometer analysis.

4. RESULTS AND DISCUSSION

4.1 Determining Required Flow Rates

Vybrant DyeCycle Orange labeled MCF7 and unlabeled MDA-MB-231 cell mixture (20.000 cells/ml) was passed through the channels and microscope images were captured and focusing of MCF7 cells was observed. Fig. 4.1 shows the focused MCF7 cells at second outlet. Red spots that seen on pictures are the artifacts form the channel. 700 μm wide channel image was captured from channel curve adjacent by starting point of outlets.

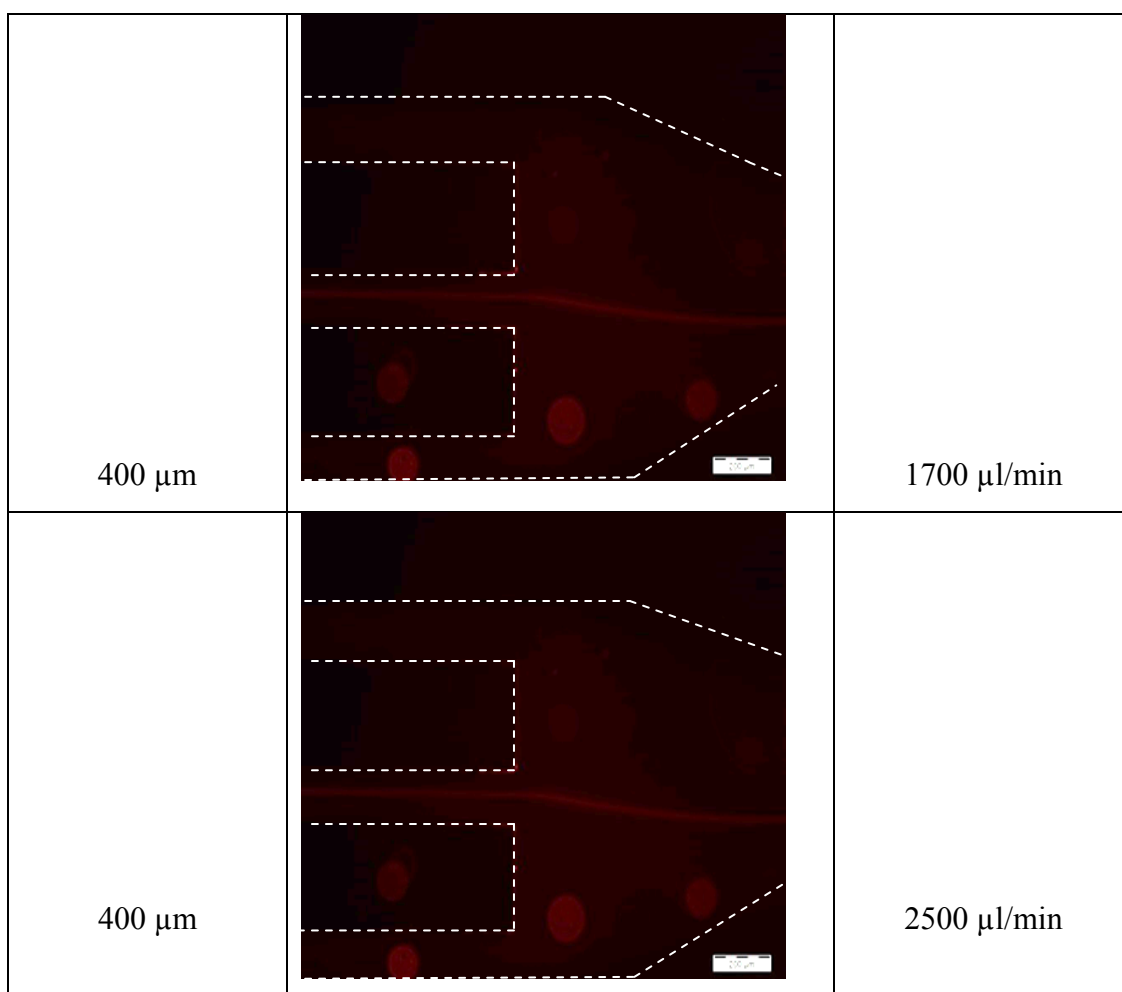


Figure 4.1 : Focus images of 400 – 700 μm wide channels due to flow rates.

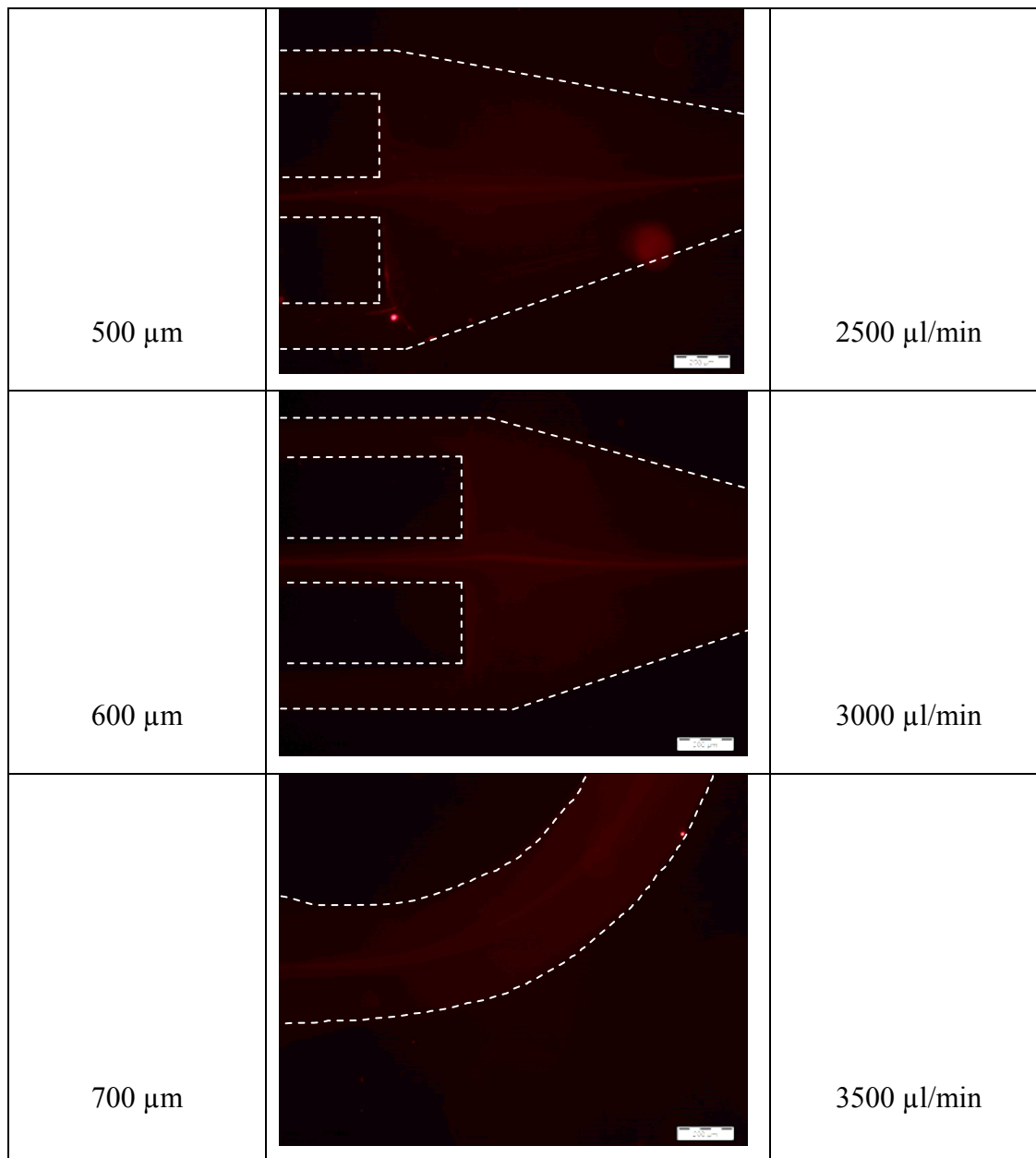


Figure 4.2 (continued) : Focus images of 400 – 700 μm wide channels due to flow rates.

Dean numbers were calculated for flow rates that are required for focusing and Table 4.1 shows the Dean numbers for each flow rate and channel.

Table 4.1 : Flow rates – Dean numbers.

Width (μm)	Flow Rate ($\mu\text{l}/\text{min}$)	D_e
400	1700	25.84
400	2500	38
500	2500	30.25
600	3000	28.78
700	3500	26.52

Collected cells from three outlets were counted by flow cytometer to confirm enrichment at second outlet. Fig. 4. 2 shows MCF7 population at second outlet is higher than other two outlets. 700 μm wide channel outlets yield comparable MCF7 amount that means there is comparatively less at second outlet.

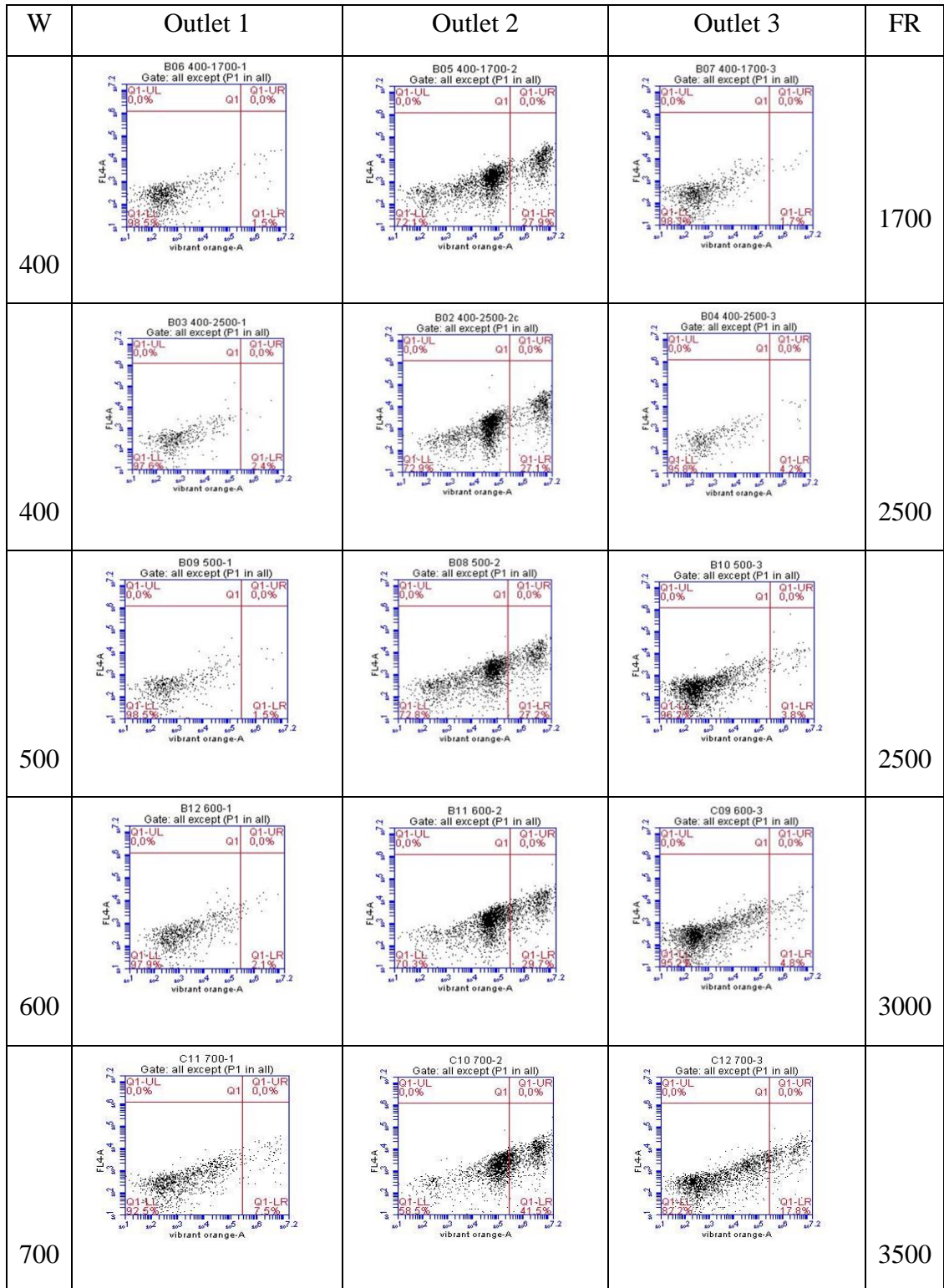


Figure 4.3 : Flow cytometer results of three outlets.

4.2 CFSE Labeled MCF7 and Unlabeled MDA-MB-231 Mixture Experiments

These experiments were done with two groups of cell mixture which are labeled with different amount of CFSE. Dye amount was higher at first group and according to flow cytometry analysis CFSE showed higher efficiency at first group than second group. This required different microscope adjustments.

4.2.1 400 μm wide channel

400 μm wide and 81 μm high channel was used at 1000, 1500, 1700 and 2500 $\mu\text{l}/\text{min}$ flow rates. Processed cells were collected for each flow rate from three outlets and analyzed with flow cytometer. Fluorescence intensities were analyzed to show whether there is focus or not. Fig. 4.3 shows the microscope images and intensities for each flow rate. Dean numbers used were 15.20 – 22.80 – 25.84 – 38, respectively.

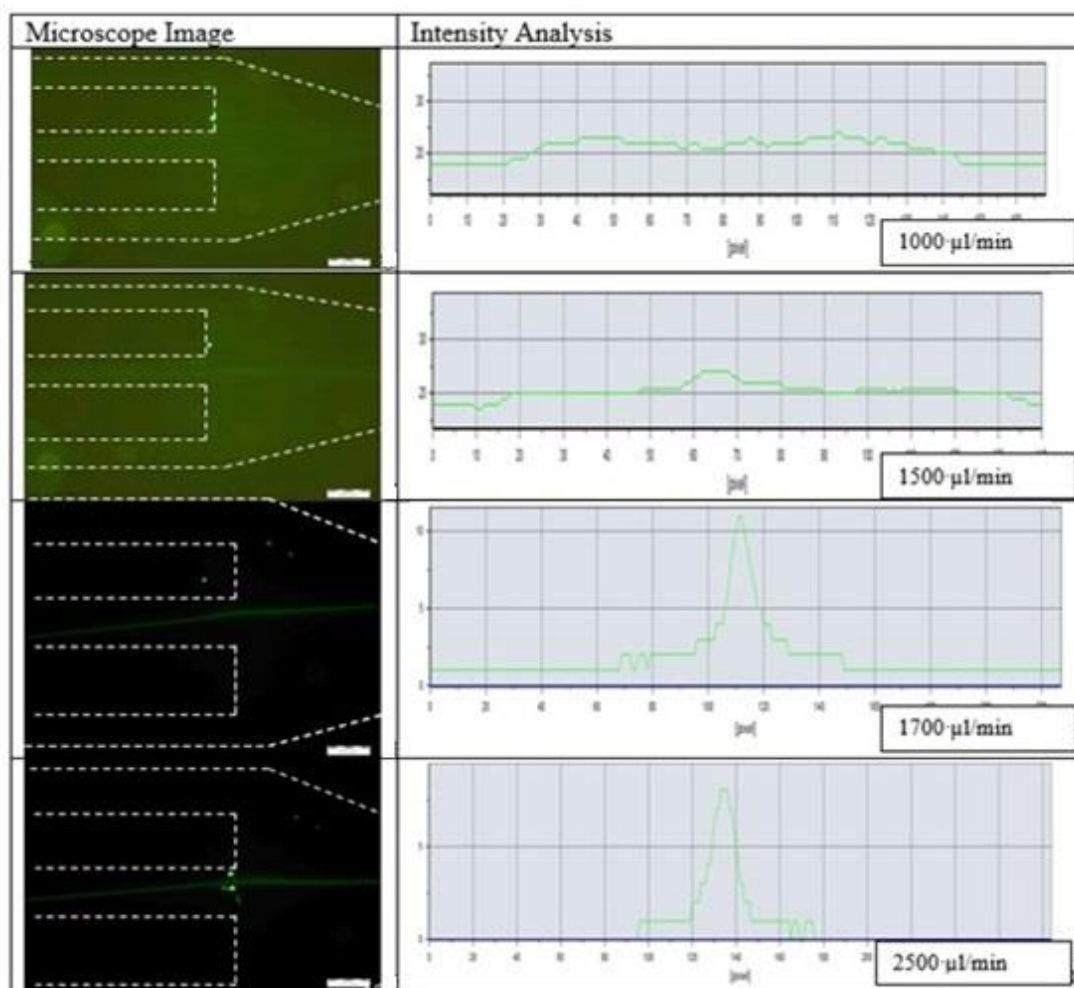


Figure 4.4 : Focus possibilities due to flow rates at 400 μm wide channel.

According to optical microscope analysis there is no focus at 1000 $\mu\text{l}/\text{min}$. At 1500 $\mu\text{l}/\text{min}$, MCF7 cells tend to equilibrate in at one direction and at 1700 and 2500 $\mu\text{l}/\text{min}$ focusing of MCF7 cells were observed. Results were confirmed with flow cytometry as shown in Fig. 4.4 at 1000 and 1500 labeled MCF7 cell percentages at each outlets are quite equal and at 1700 and 2500 percentages are much higher from at second outlet when three outlets are compared.

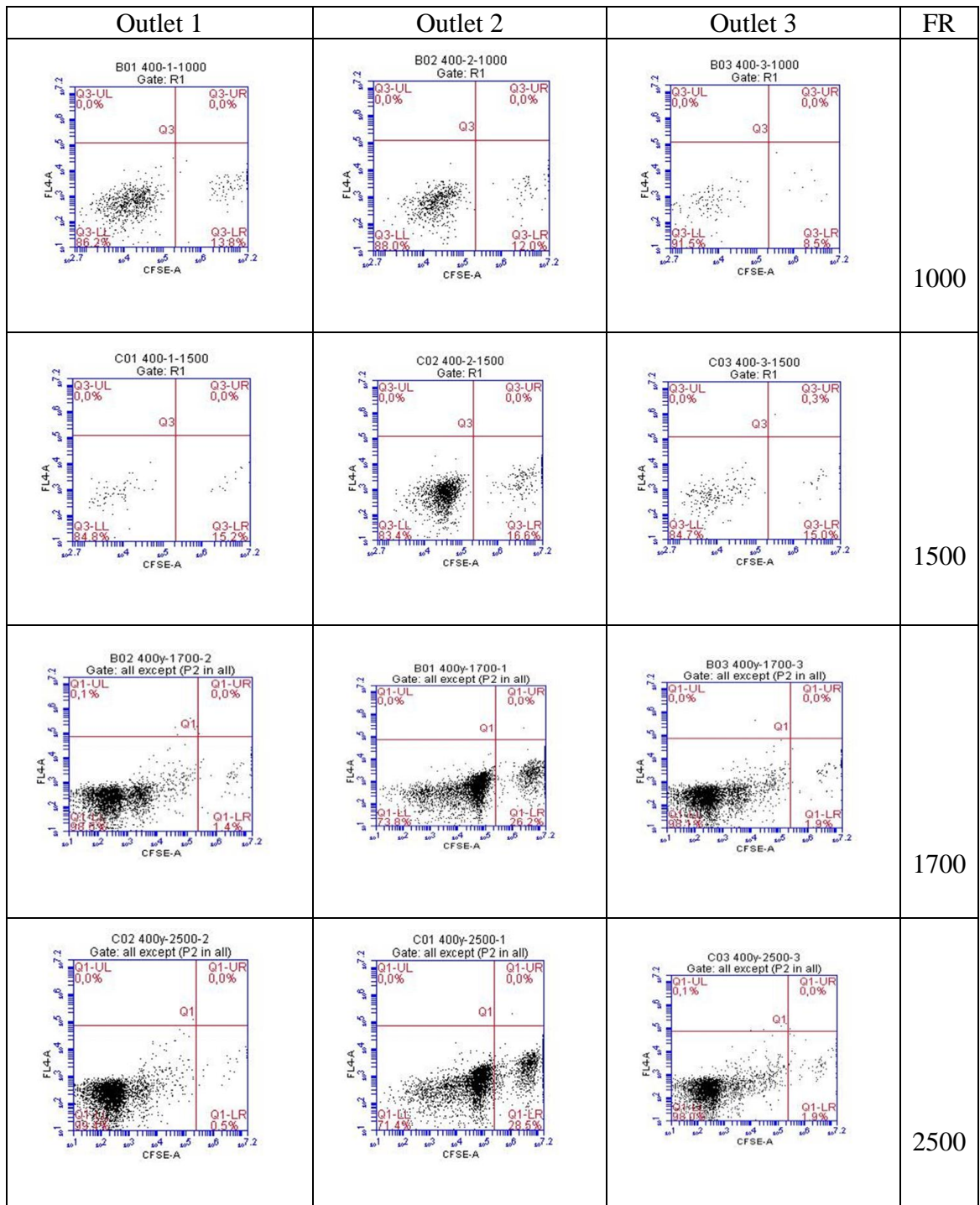


Figure 4.5 : 400 μm wide channel flow cytometer results

4.2.2 500 μm wide channel

500 μm wide and 84 μm high channel experiment was performed at 1500 – 2000 – 2500 $\mu\text{l}/\text{min}$, respectively and focus positions for each flow rate had been investigated with optical microscope images and intensity analysis. Fluorescence intensity analysis was done to show whether there is focus or not. Fig. 4.5 shows the microscope images of focused and unfocused MCF7 cells and according to optical microscope analysis there is no focus at 1500 $\mu\text{l}/\text{min}$. At 2000 $\mu\text{l}/\text{min}$ MCF7 cells tend to equilibrate in at one direction and at 2500 $\mu\text{l}/\text{min}$ focusing of MCF7 cells were observed. Dean numbers used were 18.15 – 24.20 – 30.25, respectively. Processed cells were collected for each flow rate from three outlets.

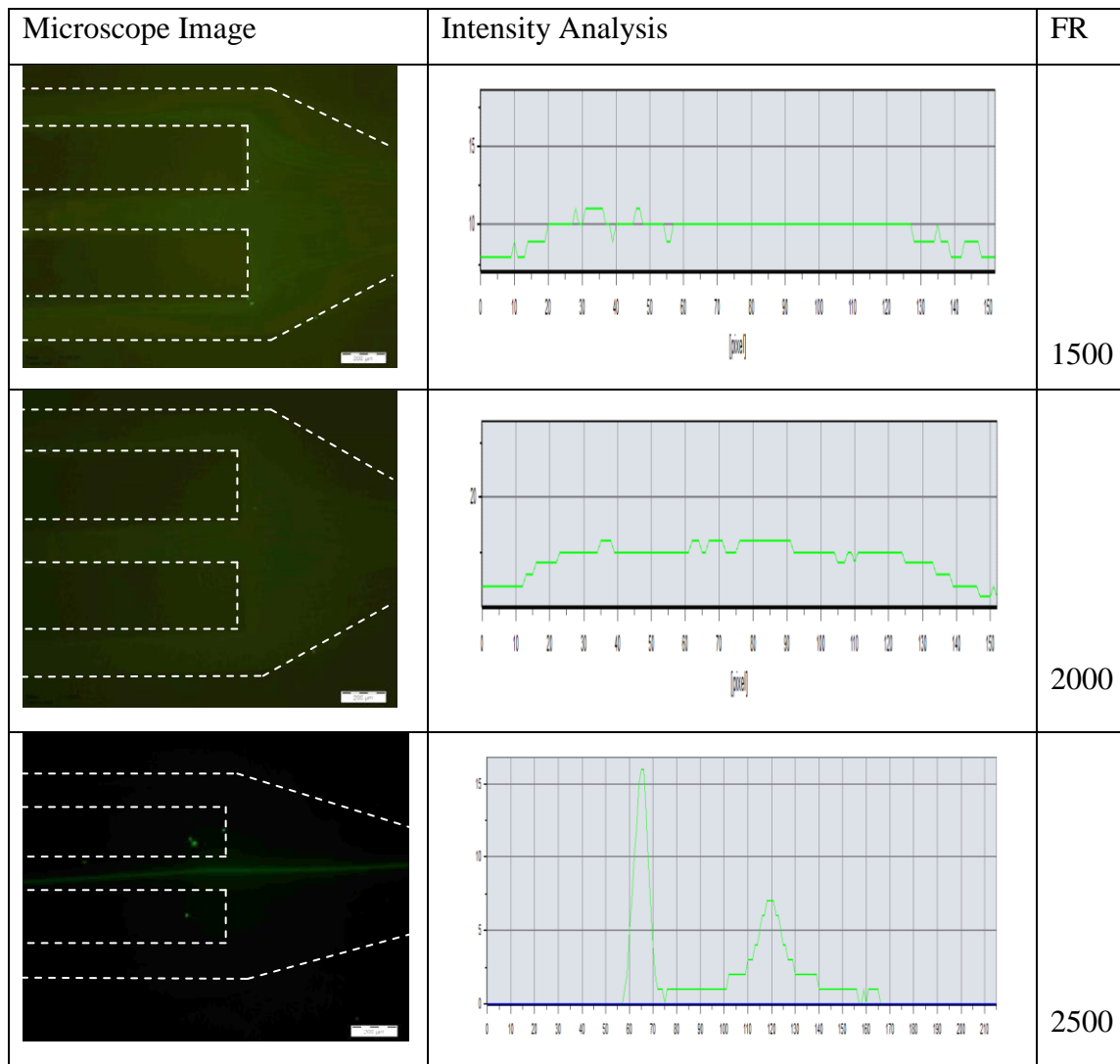


Figure 4. 6 : Focus possibilities due to flow rates at 500 μm wide channel.

Results were confirmed with flow cytometry Fig. 4.6 shows the flow cytometer results for each flow rate and at 1500 labeled MCF7 cell percentages at each outlets

are quite equal; at 2000 population in second outlet higher than other outlets but at 2500 percentages are much higher from at second outlet when three outlets are compared.

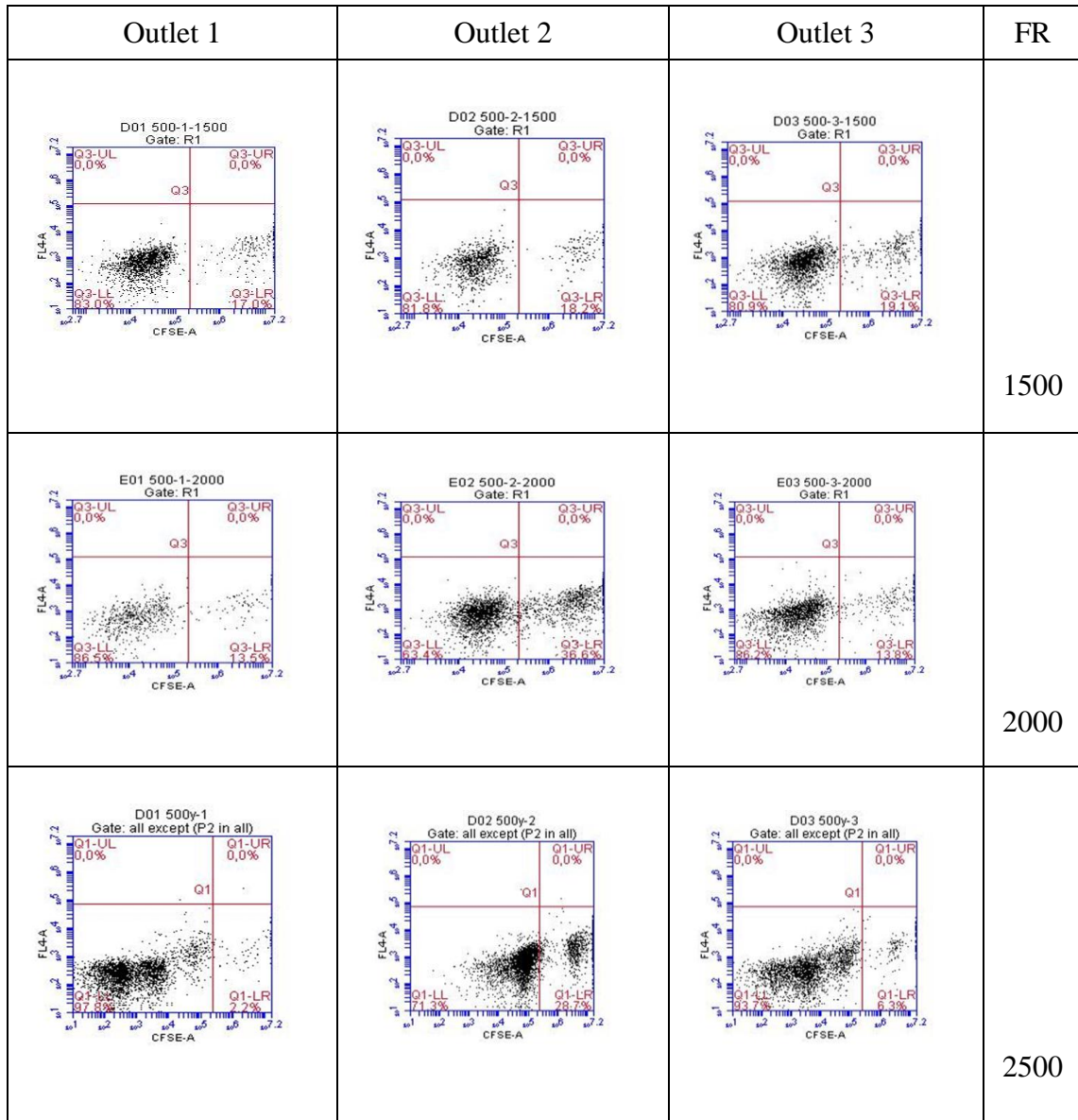


Figure 4. 7 : 500 wide channel flow cytometer results

4.2.3 600 μm wide channel

600 μm wide and 91 μm high channel experiment was performed at 2000 – 2500 – 3000 - 3500 $\mu\text{l}/\text{min}$, respectively and focus positions for each flow rate had been investigated with optical microscope images and intensity analysis. Fluorescence intensity analysis was done to show whether there is focus or not. Fig. 4.6 shows the microscope images of focused and unfocused MCF7 cells and according to these analysis there is no focus at 2000 and 2500 $\mu\text{l}/\text{min}$. At 3000 $\mu\text{l}/\text{min}$ MCF7 cells tend

to equilibrate in at one direction and at 3000 and 3500 $\mu\text{l}/\text{min}$ focusing of MCF7 cells were observed. Dean numbers are 19.18 – 23.97 – 28.76 – 33.56, respectively.

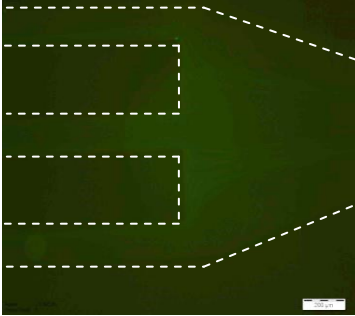
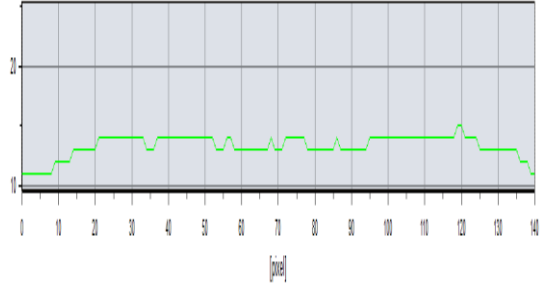
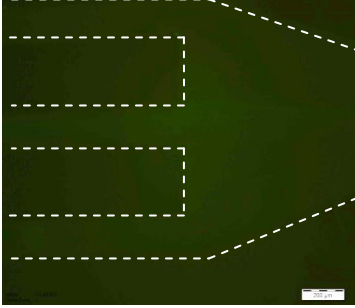
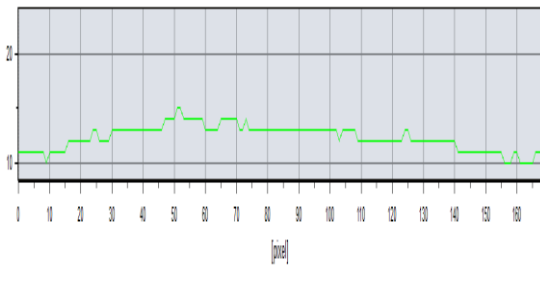
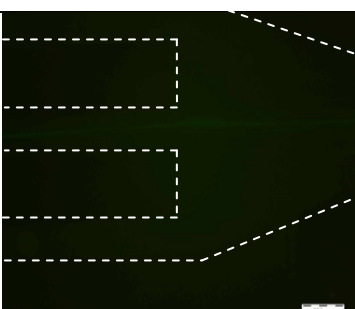
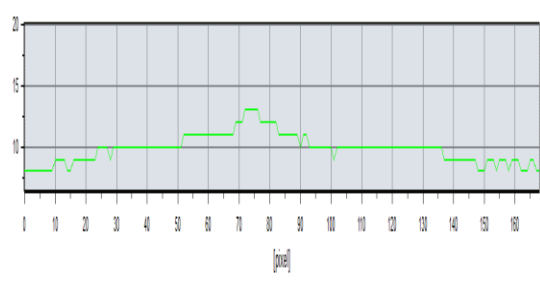
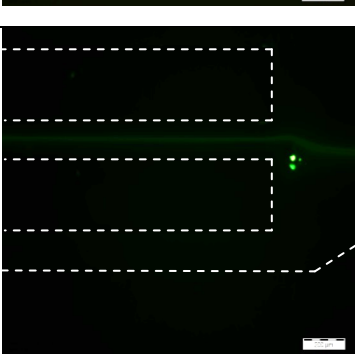
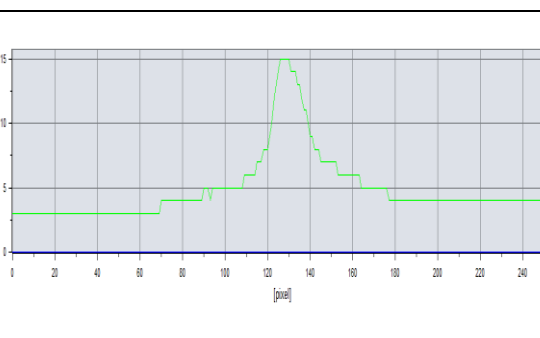
Microscope Image	Intensity Analysis	FR
		2000
		2500
		3000
		3500

Figure 4. 8 : Focus possibilities due to flow rates at 600 μm wide channel

Processed cells were collected for each flow rate from three outlets. Results were confirmed with flow cytometry Fig. 4.7 shows the flow cytometer results for each flow rate and at 2000 and 2500 $\mu\text{l}/\text{min}$ labeled MCF7 cell percentages at each outlets are quite equal; at 3000 population in second outlet higher than other outlets but at

3500 percentages are much higher from at second outlet when three outlets are compared.

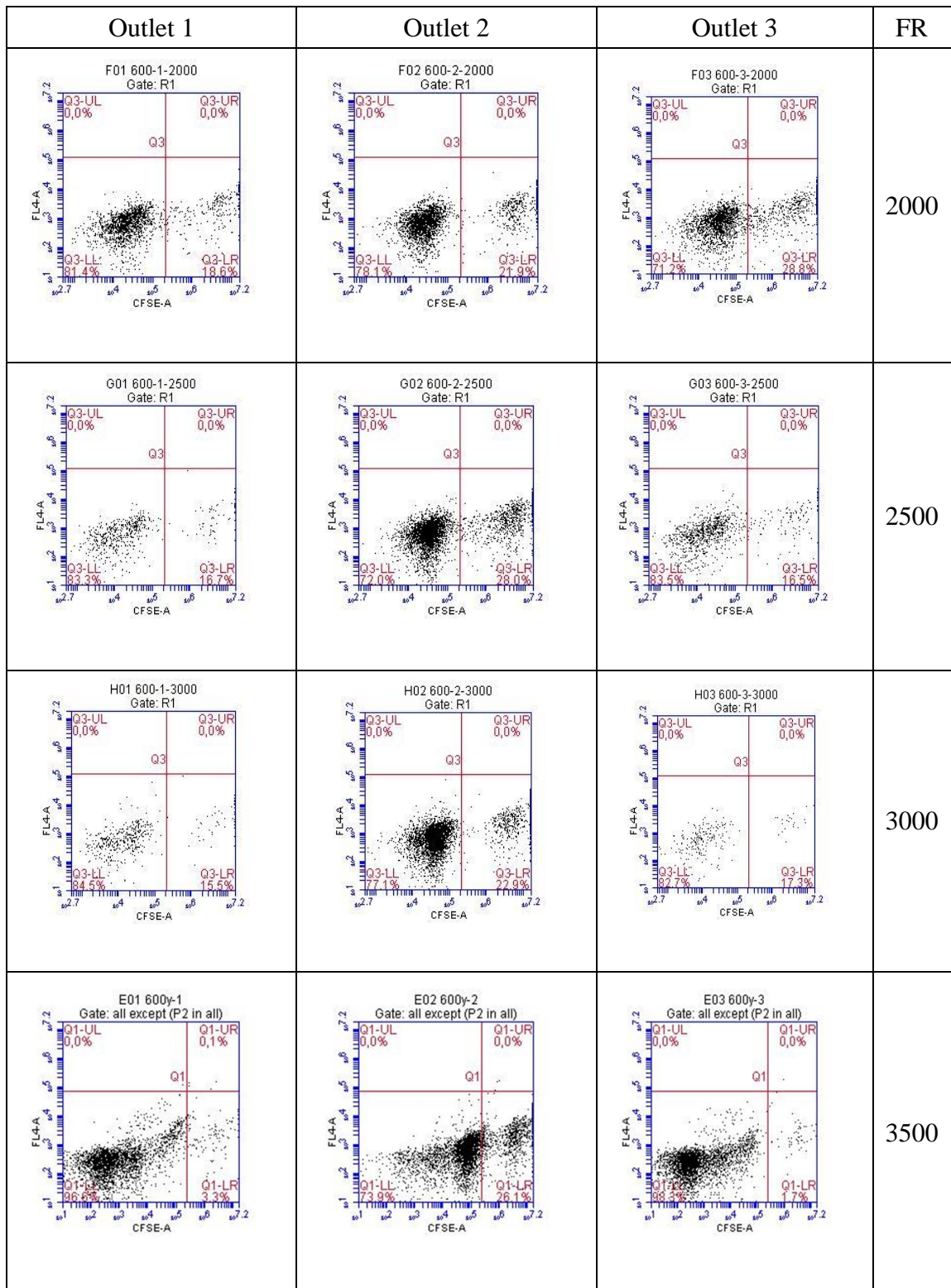


Figure 4.9 : 600 wide channel flow cytometer results.

4.2.4 700 μm wide channel

700 μm wide and 86 μm high channel experiment was performed at 2500 – 3000 - 3500 $\mu\text{l}/\text{min}$, respectively and focus positions for each flow rate had been investigated with optical microscope images and intensity analysis. Fig. 4.9 shows the microscope images and intensities for each flow rate. However no focus positions were observed for these flow rates. Flow cytometry analysis showed as in Fig. 4.10 there are MCF7 cells at each three outlets and enrichment could not be achieved. Higher than 3500 $\mu\text{l}/\text{min}$ flow rates were required to focus MCF7 cells but it was not performed due to technical problems with syringe pump.

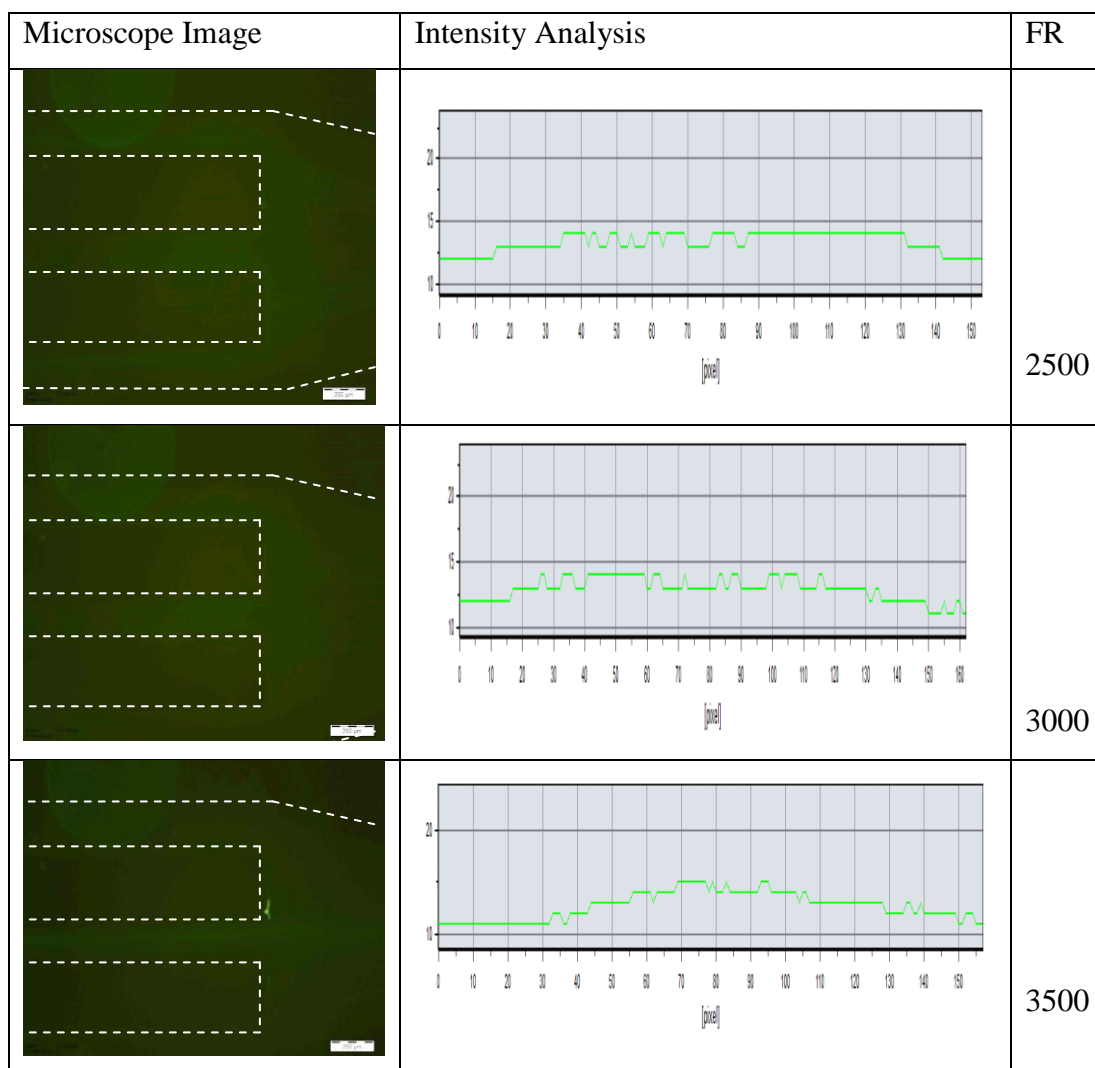


Figure 4. 10 : Focus possibilities due to flow rates at 700 μm wide channel.

Focus possibilities and positions were investigated by changing the flow rates in different designs of microflow systems. The observations show that higher flow rates, thereby higher Dean numbers, yield more efficient focus, thus such conditions

are better off in enrichment aims. Gosset and DiCarlo reported that increasing Dean numbers contribute focusing of particles in shorter distances thus it reduces the pressure in the channel and power [44].

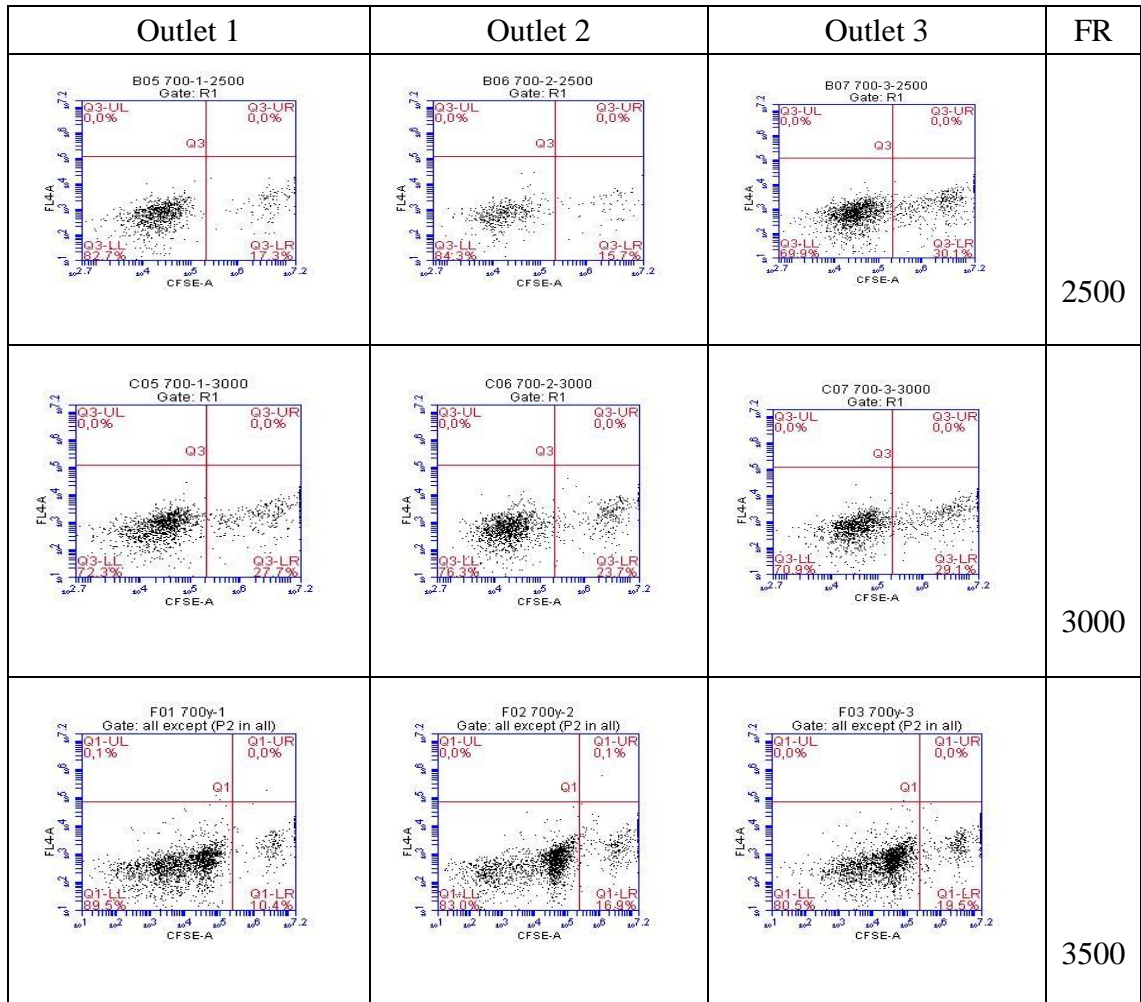


Figure 4. 11 : 700 μm wide channel flow cytometer results.

400 to 600 μm wide channels can be used for enrichment purposes at high flow rates while 700 μm channel requires higher flow rates rates contrary to the theoretical calculations. Since there is a technical difficulty for applying flow rates higher than 3500 $\mu\text{l}/\text{min}$ by syringe pump, the corresponding results were not reported here. Moreover, the flow cytometer results confirm the findings obtained in enrichment studies so that there is an enhanced enrichment at 2nd outlets of 400 to 600 μm wide channels with different flow rates as presented above.

5. CONCLUSIONS AND RECOMMENDATIONS

Early diagnosis of cancer is crucial for a patient to maintain his/her existence and for a doctor to predict the phase of the disease. More specific and precise methods are necessary for early diagnostic. These methods should be helpful for the analyzer to predict the duration, time and treatment alternatives. Conventional methods are based on the understanding of the cell morphology and investigating the tissue after biopsy and these methods are highly invasive [5].

In this work MCF7 cell enrichment possibilities were shown in curved channels having four different width and height values. Passive sorting technique was used to achieve this goal hence no external force besides syringe pump was used. This can be regarded as a big step to develop devices that are cost effective, portable or nonsophisticated for a possible cancer diagnosis. Since the detection of cancer can be performed by not using conventional techniques, patients can be protected from unnecessary surgeries. Experiments were done under 10 min. so that the time for waiting to get the pathology results can be decreased and this will lead to exact and reliable diagnosis. Microfluidic devices decreased the reagent volumes in isolated single cancer cells and enabled researches having multiple parameters. These are especially suitable to analyze small amount of cells, extracted from patient, fast and they can be used in clinical and diagnostic laboratories properly.

Experiments showed that working with higher flow rates in these curved channels gave much more focus possibilities and enrichment results. Since 700 μm wide channel did not show efficient enrichment, it can be said that channel width wider than 700 μm does not seem to be suitable for sorting purposes.

These channels were designed to achieve enrichment of one type of cells while other one remains unfocused thus collected from all outlets. However, if channel dimensions are changed a complete separation of different type of cells, individually from each outlet can be achieved. To increase portability these channels can be integrated with a micropump system which makes the experimental setup more self

sufficient. Also, biomarker and circulating tumor cell detection based researches will be useful for early cancer diagnosis.

REFERENCES

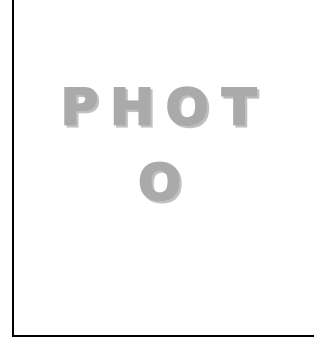
- [1] **Gross, P. G., Kartalov, E. P., Scherer, A. & Weiner, L. P.** Applications of microfluidics for neuronal studies. *Journal of the Neurological Sciences* 252, 135–43 (2007).
- [2] **Wlodkowic, D. & Cooper, J. M.** Tumors on chips: oncology meets microfluidics. *Current Opinion in Chemical Biology* 14, 556–67 (2010).
- [3] **Backhouse, C. & Gajdal, A.** Improved resolution with microchip based enhanced field inversion electrophoresis. (2003).
- [4] **Pilarski L. M., Adamia S., Pilarski P. M., Prakash R., Lauzon J, Backhouse C. J..** Improved Diagnosis and Monitoring of Cancer Using Portable Microfluidics Platforms. *Proceedings of the 2004 International Conference on MEMS, NANO and Smart Systems (ICMENS'04)* Alberta, Canada (2004)
- [5] **Tothill, I. E.** Biosensors for cancer markers diagnosis. *Seminars in cell developmental biology* 20, 55–62 (2009).
- [6] **Pamme, N.** Continuous flow separations in microfluidic devices. *Lab on a Chip* (2007).
- [7] **Chikkaveeraiah B. V., Mani V., Patel V., Gutkind J. S., Rusling J. F.,** Microfluidic biochemical immunoarray for ultrasensitive detection of two cancer biomarker proteins in serum .*Biosensor and bioelectronics* 26, 4477-4483 (2011)
- [8] **Sethu, P., Sin, A. & Toner, M.** Microfluidic diffusive filter for apheresis (leukapheresis). *Lab on a Chip* (2006).
- [9] **Ji H., Samper V., Chen Y., Heng C., Lim T., Yobas L.,** Silicon-based microfilter for whole blood separation. *Biomedical Microdevices* 10, 251-257 (2008)
- [10] **Hosokawa M., Hayata T., Fukuda Y., Arakaki A., Yoshino T., Tanaka T., Matsunaga T.,** Size-selective microcavity array for rapid and efficient detection of circulating tumor cells. *Analytical Chemistry* 82, 6629-6635 (2010).
- [11] **VanDelinder, V. & Groisman, A.** Separation of plasma from whole human blood in a continuous cross-flow in a molded microfluidic device. *Analytical Chemistry* (2006).
- [12] **Davis J., Inglis D., Morton K., Lawrence D., Huang L., Chou S., Sturm J., Austin R.,** Deterministic hydrodynamics : Taking blood apart, *Proceedings of the National Academy of Sciences of the USA*, 2006

- [13] **Zheng S., Lin H., Liu J.-Q., Balic M., Datar R., Cote R.J., Tai Y.-C.**, Membrane microfilter device for selective capture, electrolysis and genomic analysis of human circulating tumor cells. *Journal of Chromatography A* 1162, 154-161 (2007)
- [14] **Chen, D., Du, H. & Li, W.** A 3D paired microelectrode array for accumulation and separation of microparticles. *micromechanics and microengineering* (2006).
- [15] **SooHoo, J. & Walker, G.** Microfluidic liquid filters for leukocyte isolation. 29th Annual International Conference of the IEEE EMBS (2007).
- [16] **Zheng S., Liu J.-Q., Tai Y.-C.**, Streamline-based microfluidic devices for erythrocytes and leukocytes separation. *Journal of Microelectromechanical Systems* 17, 1029-1038 (2008)
- [17] **Kuntaegowdanahalli, S. S., Bhagat, A. A. S., Kumar, G. & Papautsky, I.** Inertial microfluidics for continuous particle separation in spiral microchannels. *Lab on a chip* 9, 2973–80 (2009).
- [18] **Du, Z., Colls, N., Cheng, K. H., Vaughn, M. W. & Gollahon, L.** Microfluidic-based diagnostics for cervical cancer cells. *Biosensors and Bioelectronics* 21, 1991–1995 (2006).
- [19] **Kwon, K. W. et al.** Separation of Human Breast Cancer and Epithelial Cells by Adhesion Difference in a Microfluidic Channel. 140–150 (2007).
- [20] **He, J., Reboud, J., Ji, H. & Zhang, L.** Biomicrofluidic lab-on-chip device for cancer cell detection. *Applied Physics* (2008).
- [21] **Gärtner C., Becker H. , Carstens C., von Germar F., Drese K. S. , Fragoso A., Gransee R., Guber A., Herrmann D., Hlawatsch N. , Klemm R. , Latta D., O’Sullivan C., Lopez J. R. , SmartHEALTH : a microfluidic multisensor platform for POC cancer diagnostics**
- [22] **Kim M. S. , Kim T. , Kong S.Y. , Kwon S. , Bae C. Y. , Choi J. , Kim C.H. ,Lee E. S. , Park J.K.** Breast Cancer Diagnosis Using a Microfluidic Multiplexed Immunohistochemistry Platform (2010).
- [23] **Pilarski, L. M. et al.** Sensitive detection using microfluidics technology of single cell PCR products from high and low abundance IgH VDJ templates in multiple myeloma. *Journal of Immunological Methods* 305, 94–105 (2005).
- [24] **Bang H., Yun H., Lee W.G., Park J., Lee J., Chung S., Cho K., Chung C., Han D.C., Chang J.K. ,** Microfabricated fluorescence-activated cell sorter through hydrodynamic flow manipulation. *Lab Chip* 12, 746-753 (2006)
- [25] **Liu, B., Deng, Y., Qin, B. B. & Li, Z. Y.** Application of Microfluidics Technology in Bioanalysis. *Advanced Science Letters* 4, 150–155 (2011).
- [26] **Lien K.Y., Chuang Y.H., Hung Y.,Hsu K.F., Lai W.W., Ho C.L., Chou C.Y., Lee G.B.,** Rapid isolation and detection of cancer cells by utilizing integrated microfluidic systems. *Lab Chip* 10, 2875-2886 (2010)

- [27] **Saliba, A.-E. et al.** Microfluidic sorting and multimodal typing of cancer cells in self-assembled magnetic arrays. *Proceedings of the National Academy of Sciences of the United States of America* 107, 14524–14529 (2010).
- [28] **Nagrath, S., Sequist, L. & Maheswaran, S.** Isolation of rare circulating tumour cells in cancer patients by microchip technology. *Nature* (2007).
- [29] **Bhagat, A.** Inertial microfluidics for continuous particle filtration and extraction. *Lab on a Chip*, 9, 2973 - 2980 (2009).
- [30] **Segré, G. & Silberberg, A.** The tubular pinch effect in the poiseuille flow of a suspension of spheres. *Bibl. anat.(Basel)* (1961).
- [31] **Park, J.-S., Song, S.-H. & Jung, H.-I.** Continuous focusing of microparticles using inertial lift force and vorticity via multi-orifice microfluidic channels. *Lab on a Chip* 9, 939–948 (2009).
- [32] **Carlo, D. Di & Irimia, D.** Continuous inertial focusing, ordering, and separation of particles in microchannels. *PNAS*, 18892 -18897 (2007).
- [33] **Di Carlo, D.** Inertial microfluidics. *Lab on a chip* 9, 3038–46 (2009).
- [34] **Bhagat, A., Kuntaegowdanahalli, S. & Papautsky, I.** Continuous particle separation in spiral microchannels using dean flows and differential migration. *Lab on a Chip* (2008).
- [35] **Bhagat A. A. S., Kuntaegowdanahalli S. S., Kaval N., Seliskar C. J., and Papautsky I.** Inertial microfluidics for sheat-less high throughput flow cytometry, *Biomed Microdevices.*, vol. 10. (2009)
- [36] **Ookawara S., Street D., and Ogawa K.** Numerical study on development of particle concentration profiles in a curved microchannel, *Chem. Eng. Sci.*, 61 3714-3724. (2006)
- [37] **MicroChem.** SU-8 3000 data sheet: Permanent epoxy negative photoresist
- [38] **McDonald, J. C., Duffy, D. C., Anderson, J. R., Chiu, D. T., Wu, H., Schueller, O. J. A., Whitesides, G. M.** Fabrication of microfluidic systems in poly(dimethylsiloxane). *Electrophoresis* 21, 27-40 (2000)
- [39] **Saha, A. A., Mitra, S. K., Tweedie, M., Roy, S., McLaughlin, J.,** Experimental and numerical investigation of capillary flow in SU8 and PDMS microchannels with integrated pillars. *Microfluid Nanofluid* 7, 451-465. (2009)
- [40] **Bhattacharya S., Datta A., Berg M. J., and Gangopadhyay S.,** Studies on surface wettability of poly(dimethyl) siloxane (PDMS) and glass under oxygen-plasma treatment and correlation with bond strength. *Journal of Microelectromechanical Systems* 14, 590-597. (2005)
- [41] <http://www.elveflow.com/microfluidic-reviews-and-tutorials/the-poly-di-methyl-siloxane-pdms-and-microfluidic>, March 2011
- [42] http://probes.invitrogen.com/resources/education/tutorials/4Intro_Flow/player.html, June 2013
- [43] http://flow.csc.mrc.ac.uk/?page_id=852, June 2013

- [44] **Gossett D. R., Di Carlo D.**, Particle focusing mechanisms in curving confined flows. *Anal. Chem.* 81, 8459-8465, (2009)

CURRICULUM VITAE



Name Surname: Merve ZUVİN

Place and Date of Birth: Kadıköy 14.03.1988

Address: Tütüncü Mehmet Efendi Cad. Dr. Rifat Paşa Sk. Aziz Kaya Apt. 17/17
Kat: 8 Göztepe/Kadıköy/İSTANBUL

E-Mail: merve.zuvin@gmail.com

B.Sc.: University of Kocaeli